Modeling sound propagation in a laboratory tank with open ocean models

Scott Hollingsworth

A senior thesis submitted to the faculty of
Brigham Young University
in partial fulfillment of the requirements for the degree of

Bachelor of Science

Tracianne B. Neilsen, Advisor

Department of Physics and Astronomy

Brigham Young University

ABSTRACT

Modeling sound propagation in a laboratory tank with open ocean models

Scott Hollingsworth
Department of Physics and Astronomy, BYU
Bachelor of Science

This thesis quantifies the extent to which two open ocean sound propagation models can model relative transmission loss in a laboratory tank. Measurements are taken in a lab tank and compared to open ocean model predictions. The models in this study are BELLHOP (a ray tracing model that is a part of the acoustics toolbox) [1] and ORCA (a normal mode model written by Westwood *et al.* [2]). Both models assume azimuthal symmetry and thus, are two dimensional. In an attempt to arrive at composite values for BELLHOP and better acrylic parameters for ORCA, Bayesian optimization (using the open source `bayesian-optimization` Python package) is done on the bottom sound speed and density. Using this optimization and other data processing techniques did not help improve the model-data agreement. At high frequencies (above 100 kHz) in addition to the tank being filled to 0.6 m, the model-data agreement is better, especially for ORCA. For all measurements taken, BELLHOP and ORCA are able to accurately predict the overall trend, but do not always get the correct interference pattern.

Keywords: Bayesian Optimization, Underwater Acoustics, water tank, scaled laboratory tank, BELLHOP, ORCA, open ocean sound propagation models, Machine Learning, Seabed Characterization

ACKNOWLEDGMENTS

I would like to thank the College of Physical and Mathematical Sciences and the Department of Physics and Astronomy for their emphasis on undergraduate research and allocation of funds for research assistantships. I would also like to thank the donors that make that funding available. I have learned several valuable research skills that will be very helpful in my career that I would not have learned from my classes. Seeing what I learned in class applied to research and vice versa was helpful in my education of physics and the research process.

I would like to thank Dr. Tracianne Neilsen for her support in my research. She has dedicated a lot of time to my education. She has always made an effort to meet with me frequently to discuss progress and future goals. She has also worked hard to make sure that I am successful once I leave BYU.

I would also like to thank my wife Elsie for her support in my academic pursuits! She has always placed a high value on my goals and ambitions.

Contents

List of Figures

Chapter 1

Introduction

1.1 Motivation

Modeling sound propagation in the shallow ocean is complicated due to the variability in the ocean environment, as illustrated in Fig. 1.1. To accurately model sound propagation in this environment, the altimetry and bathymetry must be known. Altimetry is how choppy the surface of the water is, and bathymetry is variation in the water depth as range increases. The number of sediment layers, their thicknesses, and their acoustic properties must also be known. Those acoustic properties include the sound speed (c), density (ρ), and attenuation (α) of the sediment. attenuation is how much the sound gets absorbed in decibels (dB) as it travels one wavelength in the sediment.

In addition to knowing the acoustic properties of the sediment, the sound speed in the water at every point must also be known. In Fig. 1.1, the black curves running from the surface of the water to the sediment are called sound velocity profiles (SVP). The axes for the SVPs are shown on the left. The leftmost SVP shows that as depth increases, the sound speed decreases until the minimum value where it starts to increase again. Sound speed gets slower as the temperature gets colder, so one explanation for that SVP could be that the water is getting colder as depth increases. In this

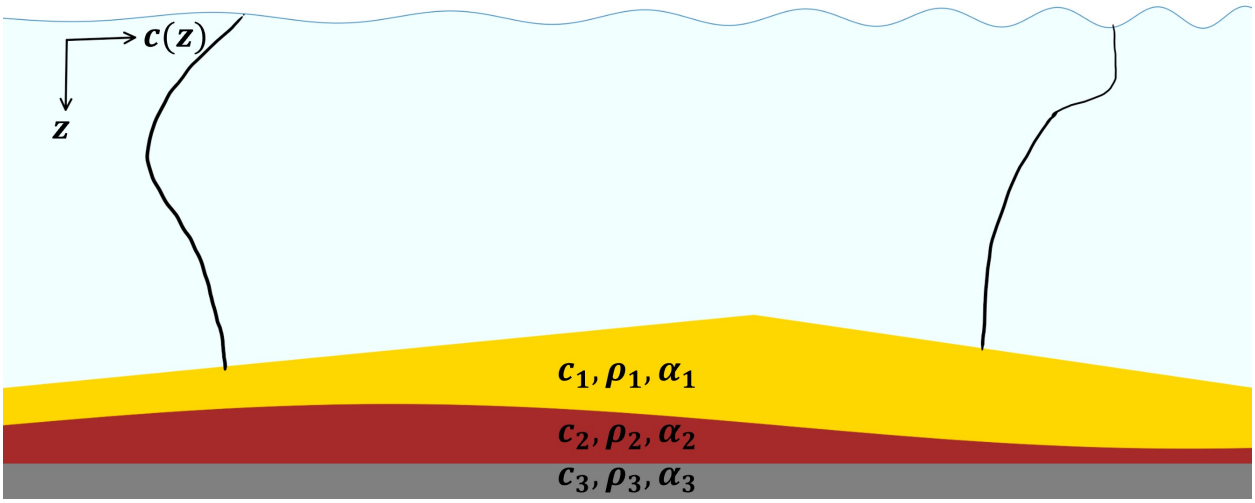

Figure 1.1 Example of a complicated ocean environment. c_i is the speed of sound, ρ_i is the density, and α_i is the attenuation of the ith layer. z is the depth.

example, warm water is rolling in on the seafloor from the left causing the water on the seafloor to be warmer than what is directly above it. The SVP on the right tells a different story. Maybe the choppier waves on the right are mixing the surface water together making it all one temperature. The warm water rolling in from the left has not made it to the right side of the environment, so the temperature (and thus the sound speed) continues to decrease all the way to the seafloor. Additional environmental complications include animal life or more complex seabeds.

Modeling sound propagation in a complex environment requires a large number of parameters which are difficult to obtain. It is unrealistic to determine all these parameters each time one desires to model sound propagation in a specific environment. Determining the composition of sediment layers is costly and time consuming. Another complication is the large spatial and temporal variability in the ocean. Considering the example in Fig. 1.1, a few hours later the wind may die down and the water surface may become smooth. The warm water rolling in from the left may have made it to the right side of the environment and changed the SVP. Because of the temporal variability, multiple measurements in one spot at different times can yield different results.

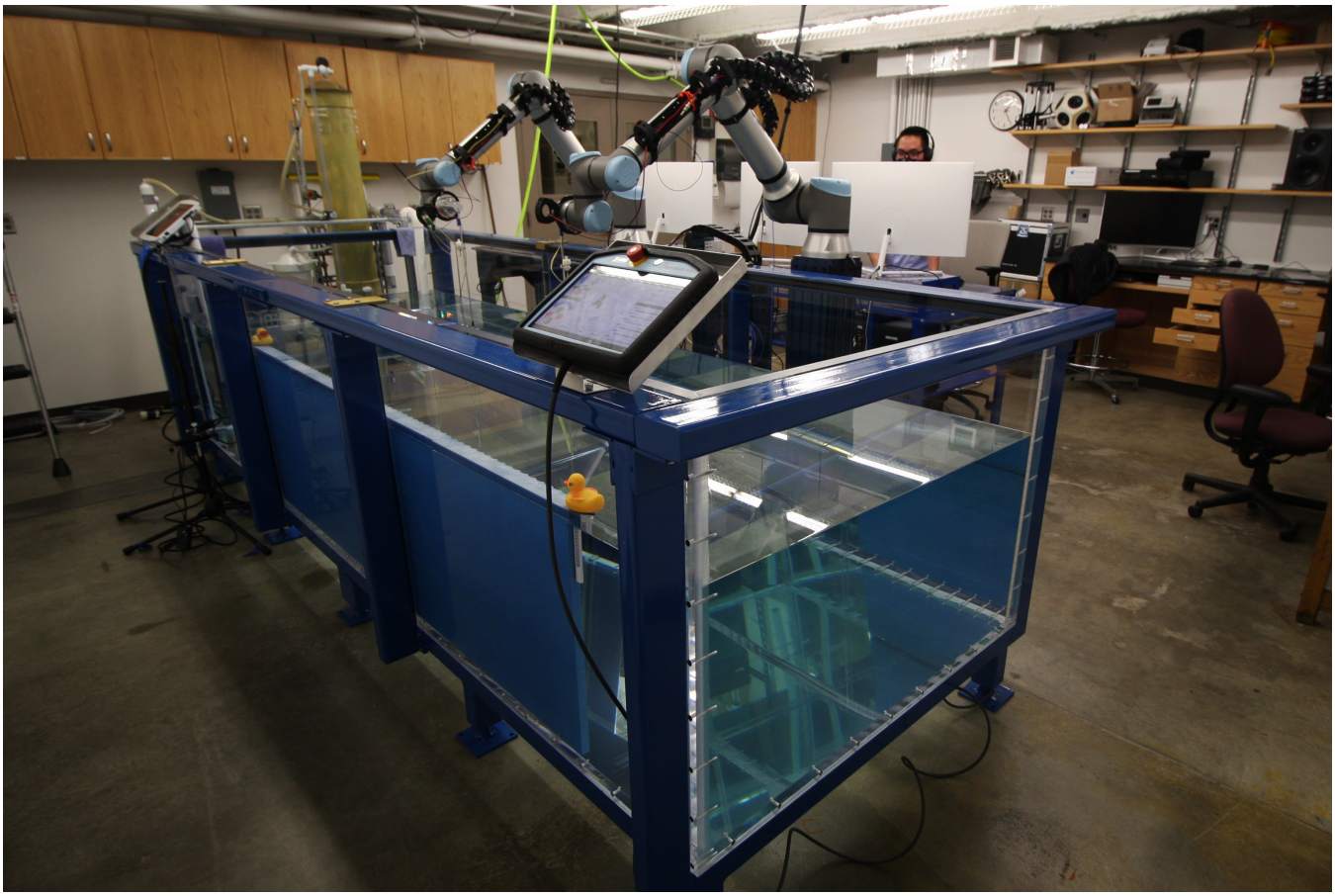

Figure 1.2 Water tank in BYU's Hydroacoustics lab. A few of the echo-reducing panels are in the tank.

These complexities are why "the acoustics of shallow water has been thoroughly investigated both theoretically and experimentally. Yet, the accumulation of theory and measurements has failed to give us the quantitative understanding required for accurate prediction of long-range propagation in shallow water." [3]

To provide a shallow water acoustic environment with more control over the parameters, an underwater acoustic water tank is used in Dr. Neilsen's research group. We can take repeated measurements with more confidence that the parameters of the environment have not changed.

1.2 Underwater Acoustic Conventions and Scaling

The key aspects of sound propagation are described by the SONAR equation: [4]

$$\mathrm{RL} = \mathrm{SL} + \mathrm{TL} \tag{1.1}$$

This equation states that the received level (RL) is equal to the source level (SL) plus the transmission loss (TL) (assuming TL<0). All these values are measured in decibels (dB). This equation says that differences in the received level from the sound source are due to TL, which is completely independent of the type of sound source.

TL is the same as the frequency response function (the Fourier Transform of the Impulse Response (IR) used in room acoustics). The TL and IR represent how the environment impacts the sound from a point source as it travels to the receiver. In underwater acoustics, both IR and TL can be used. In this research, I use TL. Transmission loss is a function of frequency, source depth, receiver depth, source-receiver range, and all the parameters in Fig. 1.1. This will be discussed more in Sec. 2.1.

In his Master's Thesis, Cameron Vongsawad calculated the IR of our laboratory tank [5]. He characterized the tank using room acoustic methods. Baumann *et al.* [6] used a small outdoor tank roughly one-sixth the size of our tank. They took measurements in the winter and let a layer of ice freeze over the top of the water. They determined how the impulse response changed if they injected oil under the ice that floated above the water. They determined that impulsive sound measurements can detect oil under ice, as the case of an oil spill in the lake or ocean. Similarities between our measurements and theirs include tank size, using a tank as a scaled model representing a large body of water, and echo-reducing material on the walls (in their case they used neoprene). One difference between the work of Baumann *et al.* [6] and Cameron's work or mine is that they measured IR in the time domain instead of TL in the frequency domain. Papadakis *et al.* [7] used a tank roughly 12 times the size of our tank. They took transmission loss measurements and compared them to

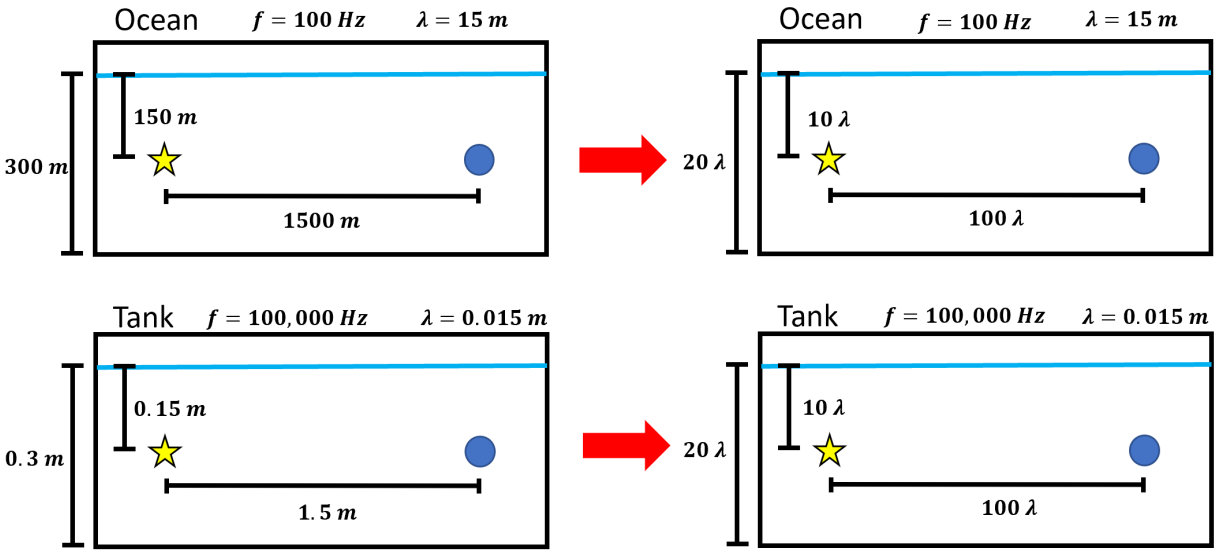

Figure 1.3 Two different environments (top and bottom) shown in two different ways (left and right). The top environment is the same as the bottom but scaled by a factor of 1000. The left half of the figure reports distances in meters while the right half reports distances in wavelengths. The star represents a source of sound while the circle represents a receiving hydrophone. Sound propagation models will report the same results for these two environments because the geometry of the problem is the same when considering wavelength.

numerical models. The work done by Papadakis *et al.* [7] is closely related to the work done for this thesis. More details of their experiment are discussed in Chapter 2.

In underwater acoustics, wavelength is a key value that helps one compare environments and define distances. When working at a single frequency, often the water depth and source-receiver range are expressed relative to the wavelengths instead of meters because the geometry of the problem depends on the wavelength. To illustrate this point, Fig. 1.3 demonstrates how two different environments can become analogous when the frequency of the sources in the two environments are chosen carefully. In Fig. 1.3, the two top environments are the same, but the one on the right reports distances in terms of wavelength instead of meters. The bottom two environments are a scaled version of the top environment when measurements are taken at a higher frequency. The

figure gives the example of a 100 Hz signal in the ocean environment on top and 100 kHz in the tank environment on bottom. The scaling is similar for any set of frequencies where the frequency used in the tank is 1,000 times greater than the frequency used in the ocean. This factor of 1,000 comes from the fact that all distances are scaled by 1,000.

Distances relative to the wavelength are also important for defining different regimes of sound propagation. For example, the water-depth-to-wavelength ratio is used to define the shallow water regime: Shallow water is defined by the depth-to-wavelength ratio between 10 and 100. [8] If the frequencies and water depths are chosen correctly, measurements in our tank can be considered shallow water measurements.

Although distances and frequencies can scale with wavelength, one limitation of scaling is that attenuation is a function of frequency. In fresh water, attenuation at 100 Hz is about 10^{-8} dB/m, but at 100 kHz it is about 10^{-2} dB/m [9]. Our tank is filled with fresh water and is only 3.6 m long. The losses due to attenuation in the tank are negligible and can be ignored. Attenuation in the sediment is much greater and, therefore, more important to consider. In the tank experiments described here, the appropriate attenuation values are represented in the models.

1.3 Open Ocean Models

To compute TL, the sound propagation models must solve the wave equation with the proper boundary conditions (due to acoustic parameters from Fig. 1.1). In her undergraduate research, Kaylyn Terry investigated using a Cartesian normal mode model to model sound propagation in our tank. This approach solves the wave equation in Cartesian coordinates (x, y, and z) and uses a sum of the normal modes to represent the sound source in the water. She based her model off of Novak *et al.* [10] who created a Cartesian model and tested it on a small glass fish tank. Her research showed that this method has limitations for our large, acrylic tank. The measured data did not follow the

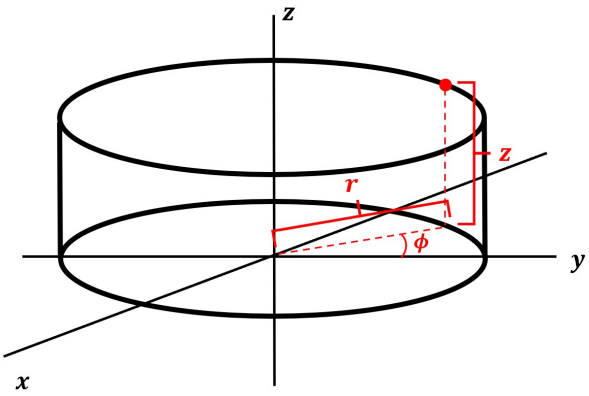

Figure 1.4 Depiction of translating from Cartesian coordinates to cylindrical coordinates.

trends of the Cartesian model's predictions. [11] The work in this thesis is similar to her research but uses open ocean models in cylindrical coordinates instead of a Cartesian tank model.

Open ocean sound propagation models commonly use cylindrical coordinates (see Fig. 1.4) to take advantage of azimuthal symmetry in environments commonly found in the ocean. Azimuthal symmetry means that no matter the value of the azimuth (ϕ in Fig. 1.4), the environment looks the same as the range increases. The solutions to the models have no ϕ dependence, thus the three-dimensional problem has been reduced to a two-dimensional one.

1.3.1 Ray Tracing

Ray tracing models create rays spreading out from the source at different angles. The model traces out the paths that those sound rays take and saves the paths that make it to the receiver. These paths connecting the source and receiver are called the eigenrays. Each time a ray reflects off an interface, acoustic energy is lost as quantified by the reflection coefficient. Ray tracing models calculate the reflection coefficients from the acoustic parameters of the water surface and seafloor. The rays also lose acoustic energy from geometric spreading. Geometric spreading results from the energy

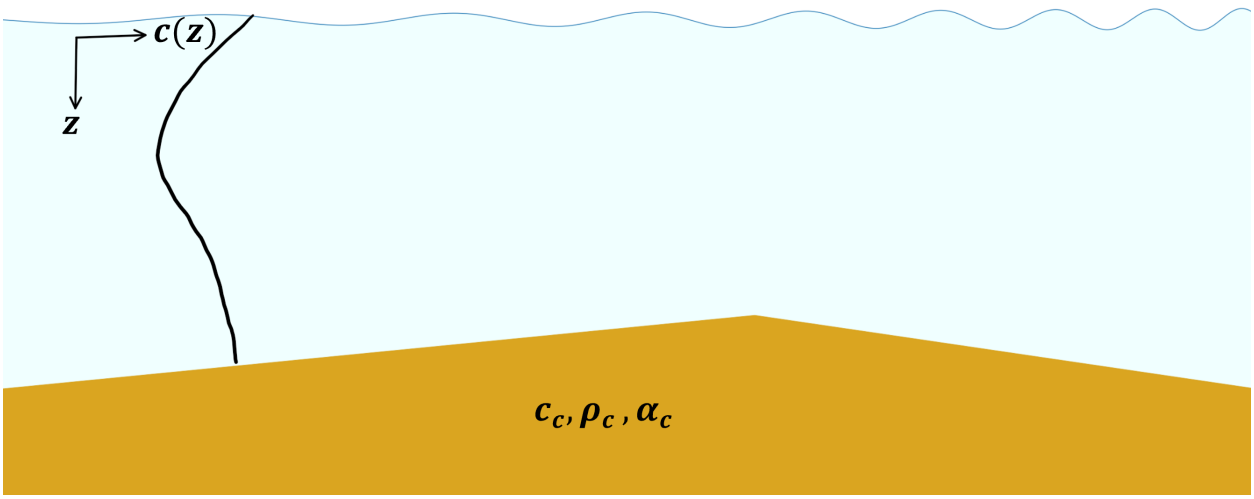

Figure 1.5 Simplified version of Fig. 1.1 representing BELLHOP. In contrast to Fig. 1.1, this model assumes c_c, ρ_c, and α_c are the composite acoustic values of an effective bottom layer or half-space.

at the sound source spreading out in all directions as it propagates. At the receiver position, the contribution of each ray to the sound field depends on the paths that ray took. A sum over all the eigenrays and other calculations yield the TL at the receiver position. These calculations can be repeated at multiple receiver locations to get the TL as a function of source-receiver range.

The ray tracing model I use is called BELLHOP [1]. This ray tracing model can handle uneven altimetry and bathymetry. In this way the model is range dependent even though it assumes azimuthal symmetry. BELLHOP assumes only one SVP for the entire environment and that the seabed can be modeled as a single effective half-space. To run BELLHOP, the complex example environment (Fig. 1.1) needs to be simplified as shown in Fig. 1.5. The parameters for the seabed are now composite values, c_c, ρ_c, and α_c, and represent the acoustic impact of the three layers in Fig. 1.1. Determining those composite values from the true layer values is not a straightforward calculation. In this work, an attempt to find them was made using an optimization technique as described in Sec. 2.4.

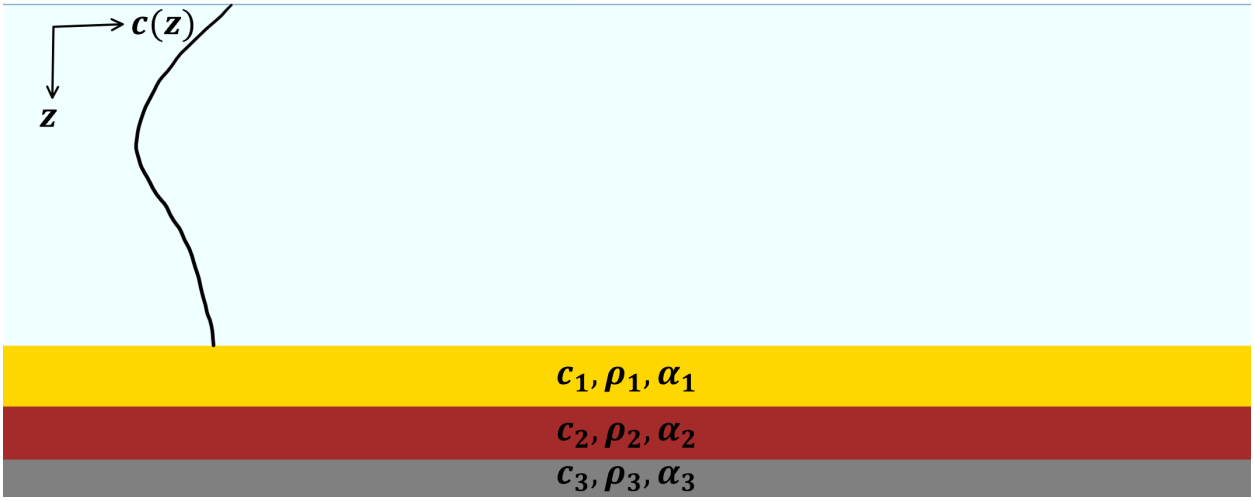

Figure 1.6 Simplified version of Fig. 1.1 representing the parameterization used in the range independent normal mode model ORCA [2].

1.3.2 Normal Mode Models

Normal mode models solve the wave equation in cylindrical coordinates taking advantage of the azimuthal symmetry. An arbitrary waveform can be represented as a sum of the normal modes, or solutions, of the wave equation based on the modal eigenvalues and depth-dependant mode function found using the seabed parameterization. The TL from the source to the receiver is obtained from a sum over these modes.

The normal mode model in this research is called ORCA [2]. ORCA is a range independent normal mode model meaning the environment must be the same as the source-receiver range increases. Range-independence requires smooth and flat bathymetry and altimetry. It also requires that the SVP is range-independent. ORCA is able to handle vertical stratification of the SVP and multiple layers of sediment. An example of parameterizing the model for ORCA is shown in Fig. 1.6.

1.4 Thesis Overview

In this thesis, I report the extent to which two open ocean sound propagation models, namely BELLHOP and ORCA, can model sound propagation in the tank. Specifically, I am investigating what frequencies, depths, and ranges yield reasonable agreement. Chapter 2 reports the methods used to take transmission loss data in the tank, the signal processing used to create transmission loss plots, the optimization process to improve model parameters, and the metrics used to compare models to data. Chapter 3 contains the results of our experiment. For several measurements transmission loss plots are shown along with tables containing correlation coefficients between the modeled and measured TL. Chapter 3 also has a discussion of the results, gives conclusions regarding what tank conditions can be best modeled with open ocean sound propagation models, and a discussion of future work on this project.

Chapter 2

Methods

The methods for determining how well the open ocean sound propagation models compare to the data measured in the tank are presented in this section. First, the experimental set-up and the measurement chain are explained. Then, transmission loss is defined and the measurements are described. The signal processing performed on the data is explained. Descriptions of the ocean sound propagation models are then provided along with the metrics for quantifying the model-data comparisons. Lastly, the Bayesian optimization process is explained.

2.1 Experimental Setup

The BYU Hydroacoustics research lab has a water tank with a sophisticated positioning system. A photo of the tank is presented in Fig. 2.1. The coordinate system is described in Fig. 2.2. The tank is 3.66 m in the y direction, 1.22 m in the x, and 0.9 m in the z. Two UR10e robots made by Universal Robotics are computer controlled to place the hydrophones in the tank with high accuracy. The robots Ægir and Rán, named after the Norse gods of the sea, are shown in Fig. 2.3. The robots can place the hydrophones to the same spot on two separate occasions with 10 micron accuracy. Even though the coordinate shift from the robot frame of reference to the tank frame of reference

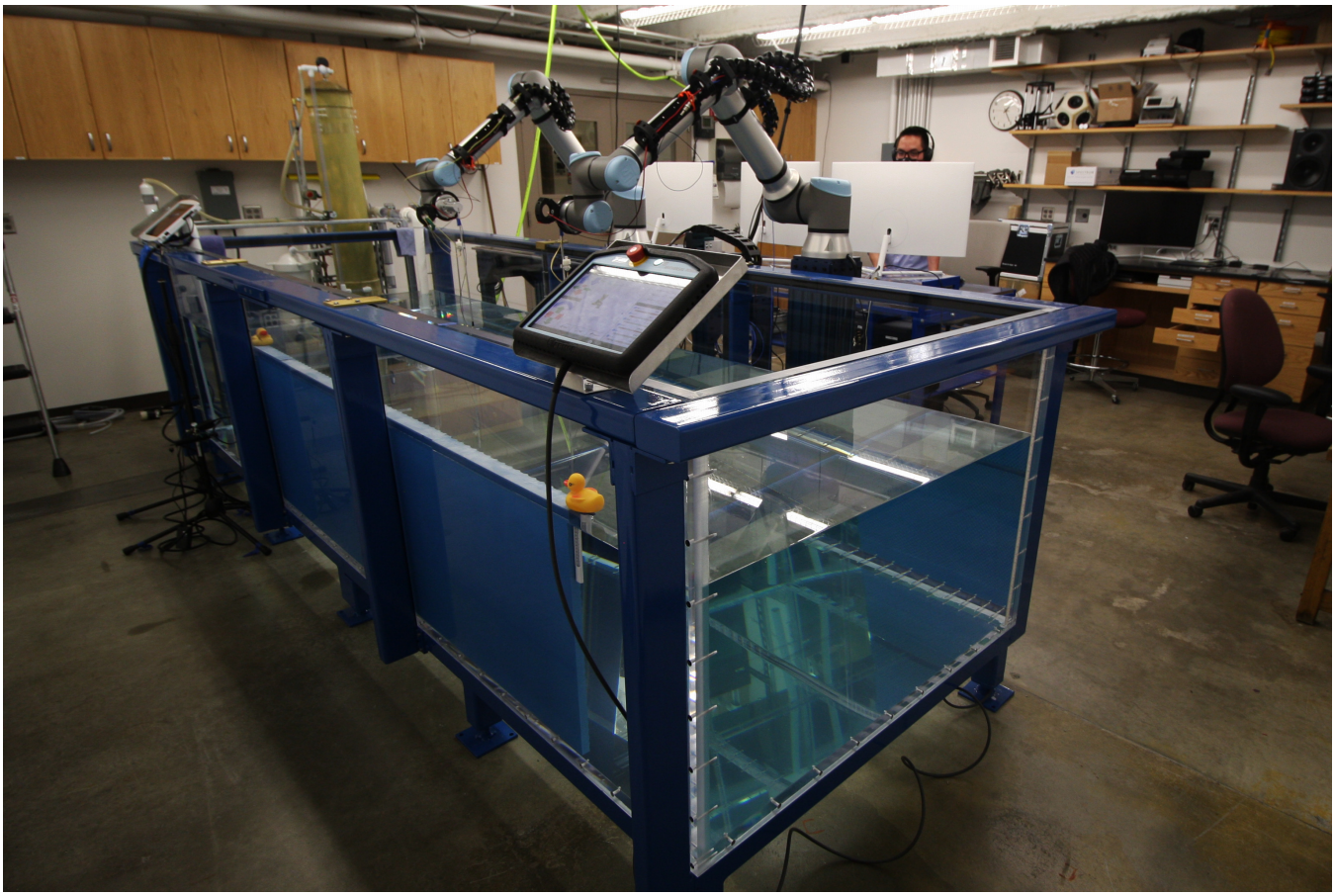

Figure 2.1 Water tank in underground lab. Some of the echo-reducing panels are in the tank.

does have an unknown uncertainty (likely on the order of 1mm), when a scan is taken twice, the hydrophones were placed in the same positions. The robots have limited range in the tank. Ægir can reach most locations in the tank if $3.66 > y > 2.14$m, and Rán can reach most locations if $0 < y < 2.06$m; Rán has greater mobility because it rests on a seventh axis extender track.

The experiments are conducted using a measurement chain designed for signals produced and received with custom LabVIEW software called Easy Spectrum Acoustics Underwater (ESAU) created by Adam Kingsley. The signal produced by ESAU is converted to an analog signal with a Spectrum M2p.65xx-x4 DAQ. That signal is then amplified with a TEGAM 2340/2350 amplifier made by TEGAM Inc. and sent to a B&K 8103 hydrophone made by Brüel and Kjær. To ensure that

the TEGAM amplified the signal correctly, a monitor signal is sent back to the Spectrum DAQ. The signal produced by the hydrophone is received by another B&K 8103 hydrophone and amplified by a B&K NEXUS Preamplifier. That signal is returned to the Spectrum DAQ and saved on the computer. As sound propagates through the tank from one hydrophone to the other, it interacts with the side walls. To reduce this effect and in an attempt to make our tank environment more closely represent an open ocean environment, the walls are lined with echo reducing tiles (Aptile SF5048 tiles made by Precision Acoustics).

In his Masters research, Cameron Vongsawad quantified the effect of the echo reducing panels using room acoustic methods [5]. In a given room, the ceiling, floor, and each wall can absorb different frequencies differently. To characterize the sound environment due to the different surface effects is to determine the spatially averaged attenuation as a function of frequency. Cameron did this for the tank with and without the panels in the tank. An average value (averaged both over space and frequency) was found to be 0.77 with the panels in the tank and 0.47 without the panels. Another value from room acoustics that can demonstrate the panels echo-reducing ability is the reverberation time (T_{60}). This is the time it takes for an impulsive sound to die down 60 dB. The T_{60} for the tank is 4.02 ms with the panels and 10.37 ms without [5].

The experimental set-up allows for a variety of measurements. For this work, comparisons need to be made between open ocean model sound propagation predictions and measured data in the tank. Transmission loss (TL) measurements as a function of source to receiver range at a single frequency are used for the comparison. These measurements are repeated for several different frequencies, source depths, receiver depths, and water depths. This helps determine the frequencies, depths, and ranges sound propagation acts like the ocean in our tank. Sound propagation models can produce a TL curve for an open ocean environment similar in scale to our tank and we can compare these modeled values with the measurements. Deeper explanation of TL is discussed in Sec. 1.2.

For the TL measurements the signal produced by ESAU is a single frequency sine wave because

ORCA and BELLHOP calculate transmission loss one frequency at a time and assume the source is a steady state signal (a sine wave). Creating an infinite sine wave for a measurement is not possible; the signal must turn on and turn off which creates a lot of high frequency noise and transient waves are produced. Both the high frequency noise and the transient waves are not desired for the model-data comparison, so the measurement must be long enough that the majority of the signal is the sine wave. Because the T_{60} is about 4 ms in the tank, the measurement does not need to be on for long for to ensure that the transient waves have died down and do not dominate the signal. For these measurements, the sine wave is on for 0.5 seconds, plenty of time to reach a steady state signal. The nature of our electronics require that we begin sampling the recorded signal before the signal turns on and after the signal is turned off. These leading and trailing values are both 0.1 seconds. These values are chosen to provide a short signal to save measurement taking time and signal processing time. The total measurement time is 0.7 seconds.

For the model-data comparisons, the hydrophone measured the sine wave at different distances from the source. For a single scan, 751 measurements are taken and each data point is at a different source-receiver range. The source depth and receiver depth are kept constant over the scan. The source-receiver range always begins at 0.1 m and ends at 1.6 m with 2mm spacing between each point in the scan. To cover the 0.1 m - 1.6 m range, Ægir was positioned at $y = 2.14$m and $x = 0.6$m, and Rán moved along the y direction from $y = 2.04$m - 0.54m and $x = 0.6$m for each. The z positions of the measurements vary for different scans. Ægir holds the hydrophone that acts as the source and Rán holds the hydrophone that receives the sound.

In addition to selecting the signal type and source-receiver range, the sampling frequency for the digital signals must be selected. The sampling frequency was chosen to be at least ten times the frequency of the sine wave for each scan. This choice ensures that when the computer produces the sine waves, it has enough data points per period to produce a smooth sine wave, and provides fine temporal resolution of the received signal.

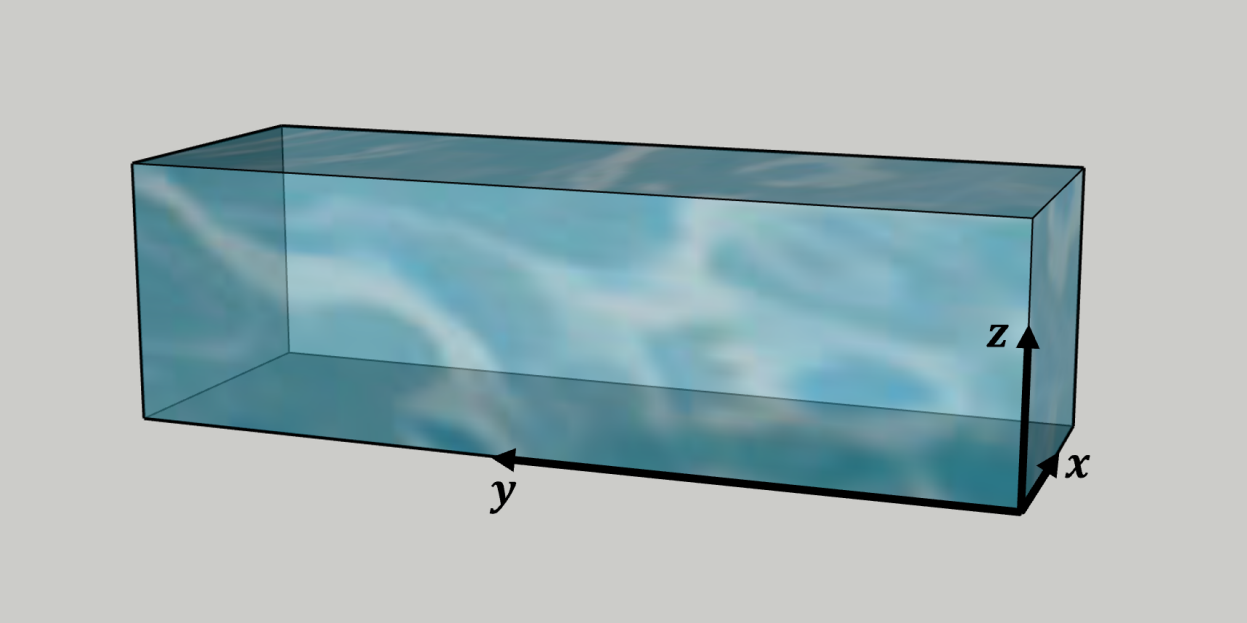

Figure 2.2 The coordinate system and origin of the tank are shown. The x coordinate points west and the y coordinate points south.

Measurements were taken at several frequencies, some corresponding to peaks or nulls in the echo reduction chart for the echo reducing panels. We hypothesize more agreement for frequencies with higher echo reduction.

At each frequency, measurements were taken with different setups. The water depth for these measurements was set to 0.6 or 0.3 m. The source and receiver were either both at a depth of one-half the water depth or with the source at one-third water depth and the receiver at two-thirds water depth. A scan was completed for many different combinations of frequency, water depth, and source and receiver depth with the echo reducing panels in the tank.

2.2 Signal processing

As described above, the received hydrophone signal is recorded and stored in units of Volts, but can be converted to Pascals using the sensitivity on the Preamplifier (10 mV/Pa). The signal can be

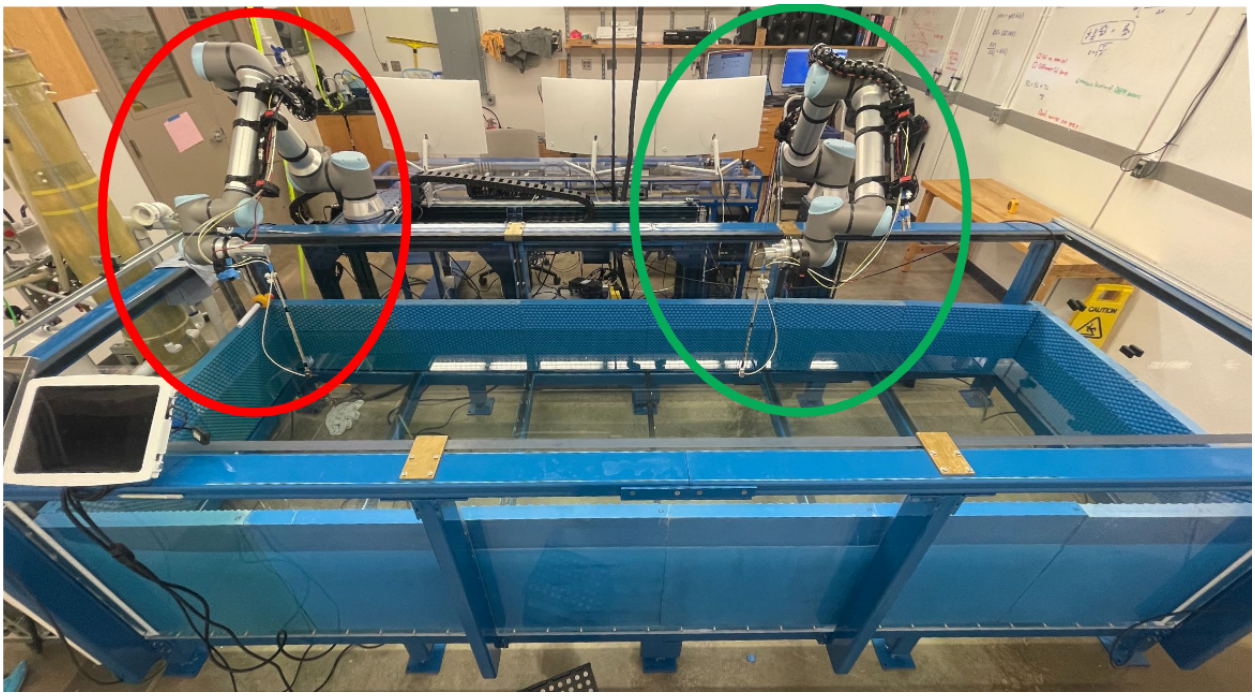

Figure 2.3 The tank is shown with the robots. The robots are referred to as Ægir and Rán (giants who live deep in the ocean in Norse mythology) with Rán on the left circled in red and Ægir on the right circled in green.

converted to decibels with the following equation:

$$\mathrm{RL} = 10\log_{10}\left(\frac{\sum_{i=0}^{N-1} x^2}{p_{\mathrm{ref}}^2}\right) \tag{2.1}$$

where RL is the received level (same RL from Eq. 1.1), x is the signal in Pascals, and p_{ref} is a reference pressure (1 μ Pa for underwater acoustics). Subtracting off SL from the RL gives TL. Assuming the SL is constant throughout the measurement, TL is often reported relative to the RL at 1 m from the source [7]. In this work TL is reported relative to the closest data point to the source (0.1 m) as was done in Papadakis *et al.* [7]. This relative TL is not true TL as described in Eq. 1.1, but it is shifted by some constant value.

The relative TL is obtained for each measurement using the following steps. The leading and trailing data (when the signal is off) are removed from the received signal to ensure that the high-frequency noise created from the signal turning on and off does not interfere with the calculations of

relative TL. Fourier analysis is done on the measurement to ensure that the electronic noise from all the measurement tools does not interfere with relative TL either. The Fourier analysis is done with our `byuarglib` Python package. A fast Fourier transform is performed, and the bin representing the frequency of the sine wave is located. Then, the 20 bins surrounding that bin are summed to ensure that any energy that leaked into other bins is accounted for. This is the summation in Eq. 2.1. The remaining calculation is performed to obtain RL at source-receiver range. The RL value at the first position (0.1 m) is subtracted off of the entire RL curve resulting in relative TL (dB re 0.1m).

2.3 Models

As described in Sec. 1.3, two open ocean sound propagation models are explored in this work. A further description of each models' parameterization and computational approach are given here.

2.3.1 Comparing Models to Data

Once the relative TL is calculated, I can compare it to the predictions made by BELLHOP and ORCA based off of the acoustic parameters of the tank bottom and the water. Acoustic parameters of the acrylic were found at NDT.net [12]. I compare the predictions to the data by calculating the Spearman ρ correlation coefficient using the `scipy.stats` Python package. This Spearman correlation is well suited for TL because it is non-parametric, and correlation is computed based on rank order. The rank order means that deep nulls present in modeled TL, but not measured TL, do not impact the correlation. Other correlation metrics would penalize the coefficient because one data set has deep nulls while the other does not. Whether ρ is calculated from TL curves in Pascals or dB, it gives the exact same result. The Pearson correlation gives a different value even though this is a simple unit conversion. Another metric was calculated to measure model-data agreement called the mean absolute error (MAE). The MAE was chosen to be a second metric because it is

calculated in a different way than the correlation coefficient, so it can be a second check. The MAE is calculated by subtracting the model curve from the measured curve, taking the absolute value, and finding the average of all the points in the new array. Explained simply, the resulting value is how many dB apart the two curves are on average. The closer to zero, the better the model-data agreement. One drawback to this metric is that it amplifies the deep nulls that occur in the modeled curves.

2.3.2 Optimization

As mentioned in Sec. 1.3.1, the composite acoustic parameters for an effective single layer are not straightforward to calculate. To approximate these values for BELLHOP, I used Bayesian optimization via the `bayesian-optimization` Python package. To use the optimizer, one creates a function that, when maximized, returns the best model-data agreement. Optimization was done on both MAE and ρ to see which resulted in a better fit to the measured data. Optimizing on the MAE resulted in a better fit so that is what is reported in this thesis. The Spearman ρ values are still calculated as a second check against the MAE, but the function of the optimization returns the MAE. The optimizer finds the parameters that maximizes this function. Because a better fit results in lower MAE, the sign of the MAE is flipped in the function. Two different optimization codes were created: one for BELLHOP and one for ORCA. The variables of the maximizing function are the density of the sediment (ρ) and the sound speed of the sediment (c). Originally the attenuation (α) of the sediment was a variable in the maximizing function, but it did not affect the maximizing function much, so was removed in order to focus the computing power on finding the other two parameters.

The maximizing function calculates transmission loss with BELLHOP (which assumes that c and ρ are composite values representing the acrylic, air gap, and concrete all in one). The function picks values within set bounds for both parameters then uses BELLHOP to calculate transmission

loss based on those parameters.

The maximizing function involving ORCA is similar to the BELLHOP function, but the acoustic parameters represent different values. ORCA can handle multiple layers of sediment, so we put the three layers of our tank as the acrylic bottom, the air gap, and the concrete below the tank. The acoustic values for air and concrete are well-known, but acrylic values can vary depending on the type. Only one source of acrylic values were found (see ndt.net [12]). So, ORCA's optimizing function attempts to find values closer to the acrylic for our tank. If the optimizations at different frequencies and source and receiver configurations converge to the same parameters for acrylic, then we can conclude some acoustic parameters for the acrylic that specifically makes up our tank bottom.

The Bayesian optimization on ORCA does not converge to the same values for different test cases, so we viewed the MAE as a function of ρ and c on a density color plot for all our different test cases. Common parameters that resulted in low MAE are found manually by looking at these plots. All these plots are displayed in Appendix B.

Chapter 3

Results

This section displays the results of the measurements, modeled predictions from BELLHOP and ORCA, and model-data agreement resulting from Bayesian optimization. The results are discussed pointing out areas of possible improvement. The future work of Dr. Neilsen's research group on this topic is discussed.

3.1 Model-data comparisons

This section provides the results of the measurements described in Chapter 2. A description of the results is provided with some discussion of the metrics used to compare. The metrics are explained in greater detail in Sec. 2.3.

3.1.1 Relative TL results

Plots of relative transmission loss as a function of source-receiver range are shown in Figs. 3.1, 3.2, and 3.3. The models are shown in blue with the measured data shown in orange. The y-axis label was removed to show the frequencies of the measured TL curves. Each grid line represents a 5 dB

change. All TL curves start at 0 dB. The water depth is $h_w = 0.3$ m, the source depth is $z_s = h_w/3$, and the receiver depth is $z_r = 2h_w/3$ for the results shown in Fig. 3.1. $z_s = z_r = h_w/2$ for both Figs. 3.2 and 3.3 with $h_w = 0.3$ m and $h_w = 0.6$ m, respectively.

We want to know the ranges that BELLHOP and ORCA work best to model the measured TL. Looking over Figs. 3.1, 3.2, and 3.3, both BELLHOP and ORCA successfully capture the overall trend of the TL data, but the destructive interference is not captured at the correct ranges. In most cases, there are short sections where the model-data agreement is good. After changing the displayed ranges to units of water depths and wavelengths, no trend was found for specific ranges that always have good model-data agreement. For certain cases, such as 53 kHz and 0.6 m water depth, both BELLHOP and ORCA seem to match with the measured data for the first 10 cm of the measurement. The measured echo reduction of the side panels (echo reducing values in dB are listed for nine frequencies in Figs. 3.4, 3.5, 3.6, and 3.7) was done at normal incidence, so it could be that they work best at normal incidence. Whereas at oblique incidences they may reduce reflections poorly. For the first 10 cm of the measurement the side reflections are closest to normal incidence, so this could be a possible explanation. The data has been analyzed in units of wavelength and water depth, but no strong patterns for which ranges work best were found, so those results are not included in this work. Both the Bayesian optimization results and the ORCA parameters chosen based off of a low MAE for all measurements do result in similar TL curves and do not provide any insight on what source-receiver ranges provide best model-data agreement. So, those results are not shown in this section but are included in Appendix B.

3.1.2 Metrics for model-data agreement

A more objective look at the data is found in the tables in Figs. 3.4, 3.5, 3.6, and 3.7. These tables report the metrics for nine different frequencies in three different measurement setups (27 measurements total). The mean absolute error (MAE) always reports lower on the models after

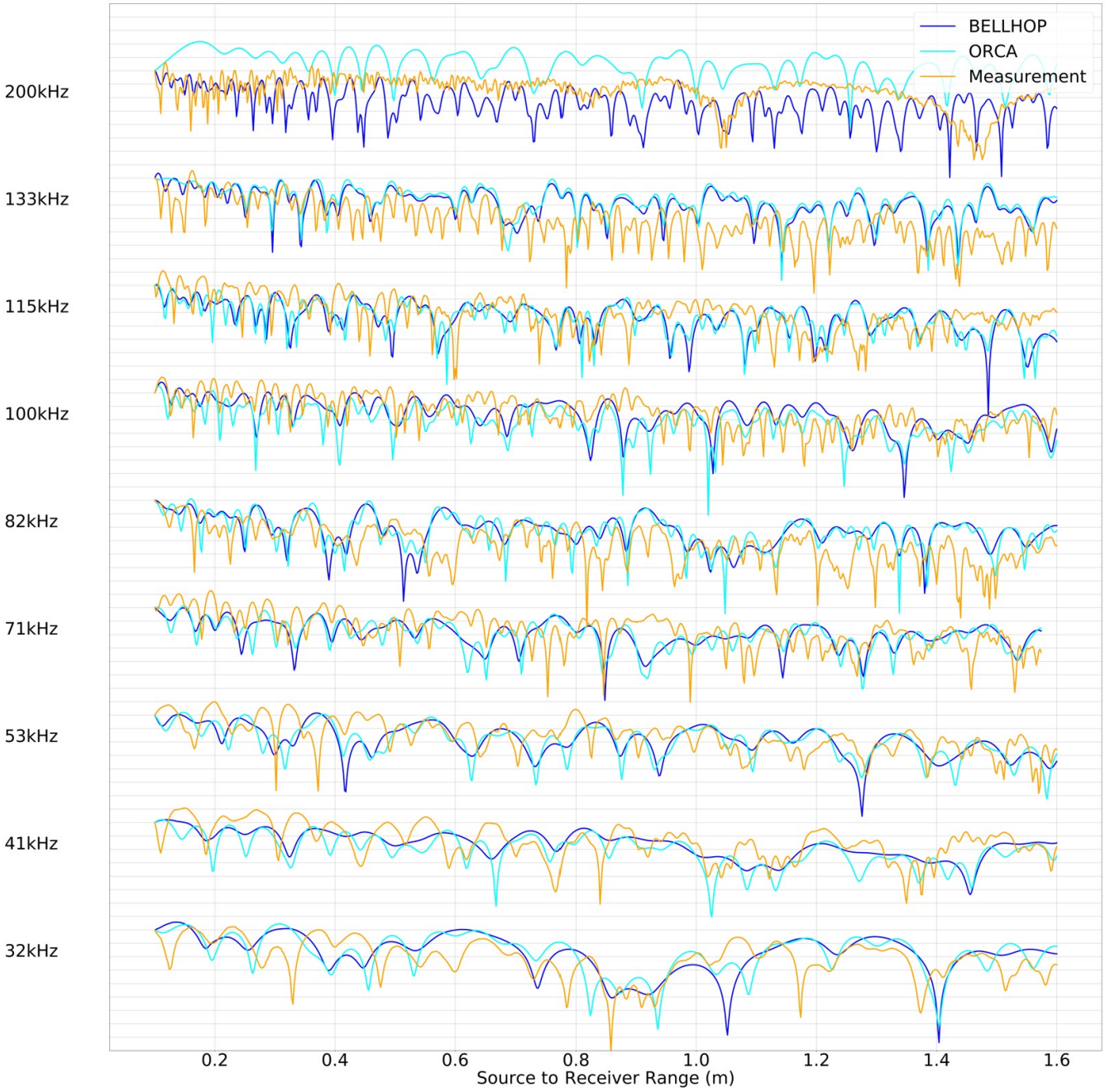

Figure 3.1 Transmission loss data sorted by frequency data for $h_w = 0.3$ m, $z_s = h_w/3$, and $z_r = 2h_w/3$. Acrylic values from ndt.net [12] are used for the c and ρ parameters for BELLHOP and ORCA. Gridline separation corresponds to a 5 dB drop in relative transmission loss. The TL curves are relative to the first position of the scan (0.1 meters).

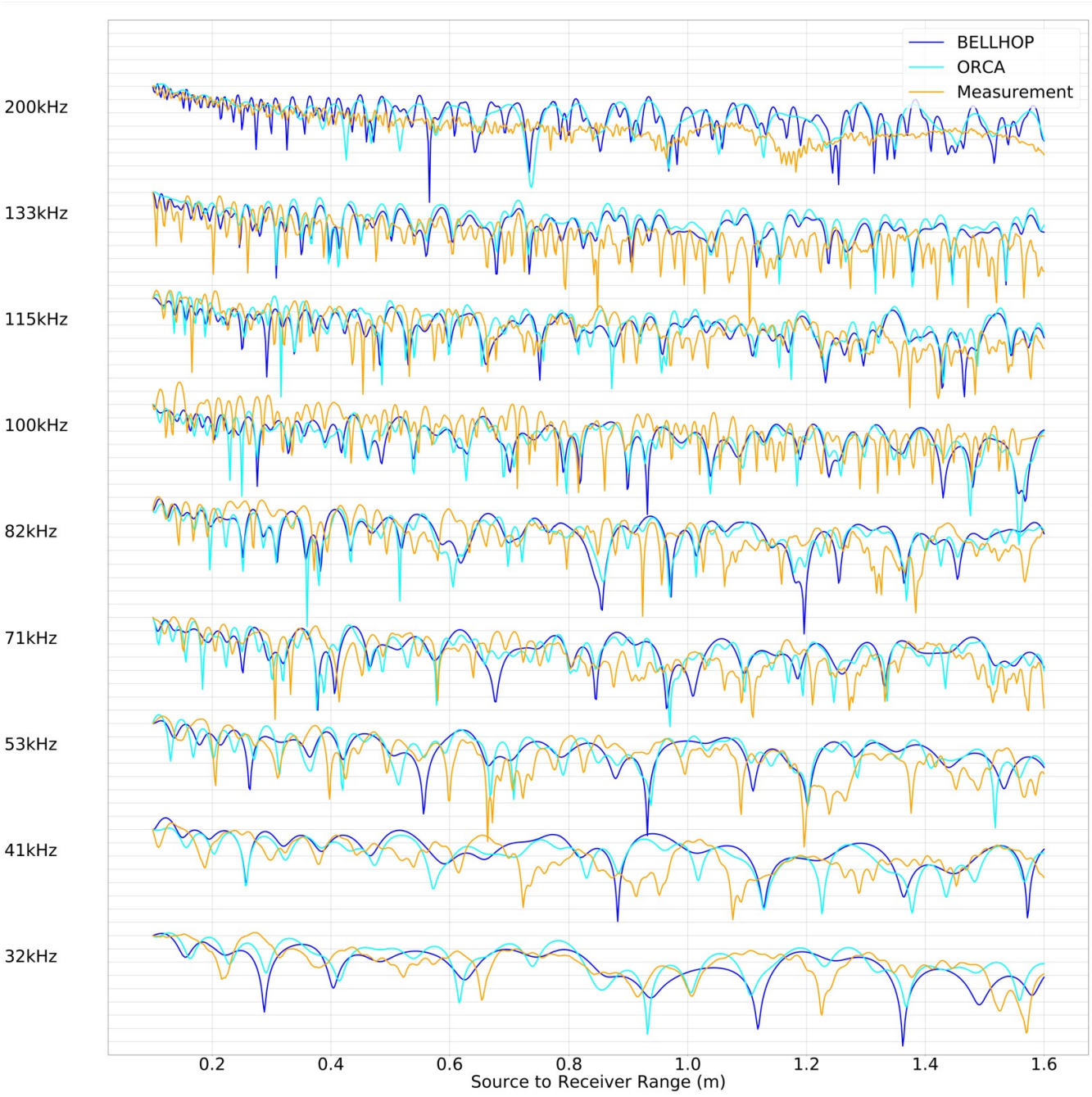

Figure 3.2 Transmission loss data sorted by frequency data for $h_w = 0.3$ m and $z_s = z_r = h_w/2$. Similar to Fig. 3.1.

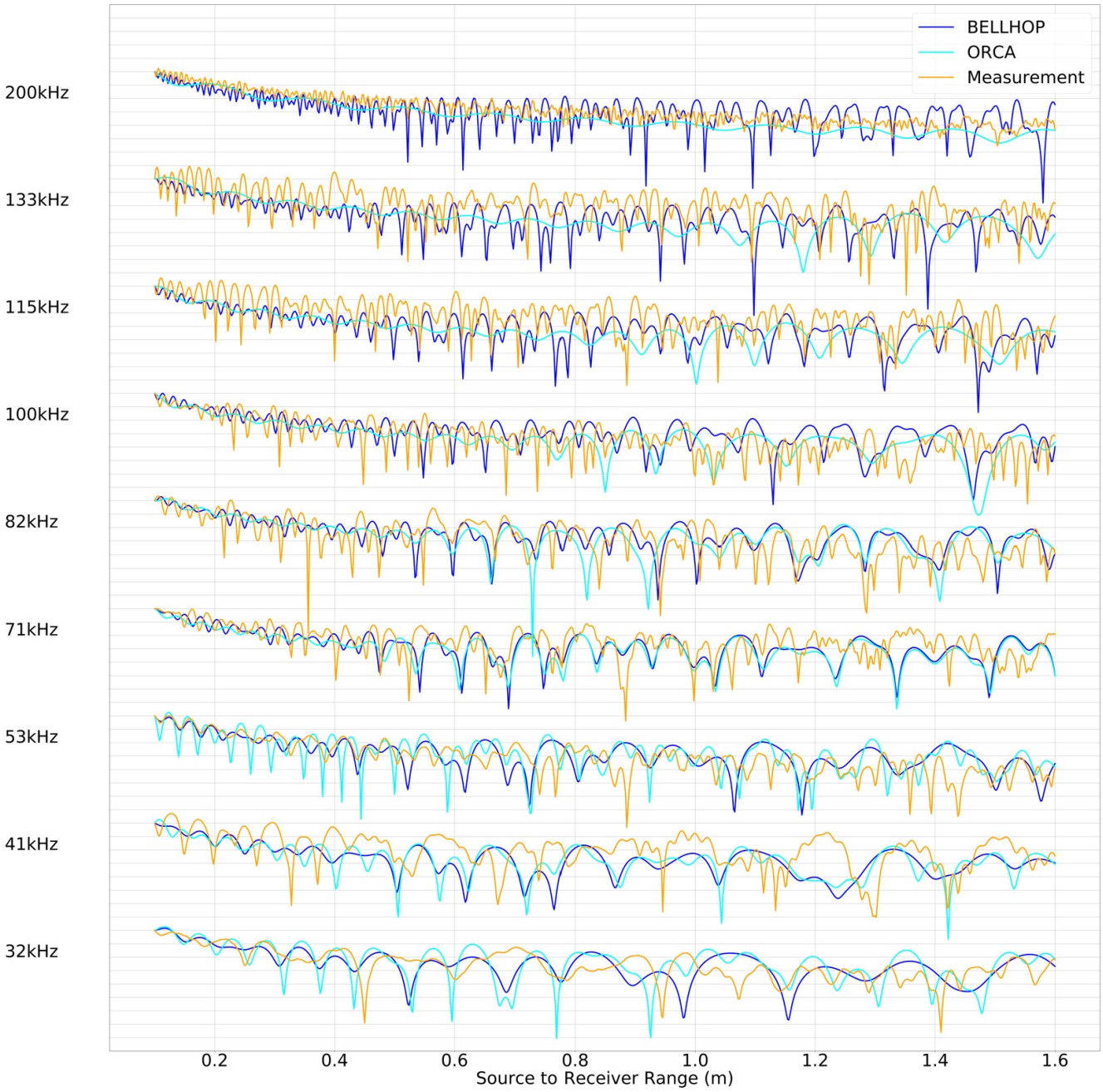

Figure 3.3 Transmission loss data sorted by frequency data for $h_w = 0.6$ m and $z_s = z_r = h_w/2$. Similar to Fig. 3.1.

Bayesian optimization because the parameters were optimized on the MAE. The Spearman ρ correlation coefficient is a second parameter to verify that the optimization improved model-data agreement. In almost all cases, the optimized model parameters give a TL curve that is more correlated with the measured data than the acrylic parameters. The only issue with this is that the Bayesian optimization does not tend towards similar parameters for different frequencies. The optimization tends to push the parameters towards the boundaries, but it is seemingly random whether those are the upper or lower bounds.

We decided to view the MAE as a function of both sound speed (c) and density (ρ) on a color density plot (see Appendix B for a comprehensive list of all density plots). After looking for trends, it was determined that $c = 2200$ m/s and $\rho = 1.8$ g/cm^3 give a TL curve that has a low MAE across all frequencies and setups for ORCA. No trends were found with BELLHOP. Because BELLHOP uses composite lower half-space parameters, the acrylic is a set thickness, and attenuation is a function of frequency, it is feasible that these composite c and ρ parameters could be a function of frequency. Three measurement setups with frequency held constant was not sufficient to see any trends, thus ORCA is the only model with reported common parameters. The common parameter metrics are sometimes better than the acrylic and sometimes worse, so this method did not seem to improve model-data agreement in any significant way.

There are no significant trends in the metrics with the echo reducing panel loss. It does not appear that higher, normal incidence echo reduction leads to better azimuthal-model-data agreement. There appears to be a trend with water depth especially at high frequencies. The model-data agreement seems to be best when water is deep as well as frequencies above 100 kHz, especially for ORCA, because the Spearman ρ values are higher and the MAE values are lower.

BELLHOP and measured data mean absolute error (dB)							
Frequency (kHz)	Panel loss (dB)	0.3 m, offset		0.3 m, same		0.6 m, same	
		Acrylic	Optimized	Acrylic	Optimized	Acrylic	Optimized
32	34	5.7	4.7	5.0	4.2	4.4	4.4
41	37	5.0	4.8	5.6	5.0	6.6	6.2
53	37	5.5	5.3	6.0	5.5	4.8	3.9
71	40	5.4	5.1	6.0	5.2	5.0	4.8
82	24	7.0	5.3	6.6	5.9	5.2	5.0
100	32	5.3	4.9	6.3	5.8	5.6	4.5
115	43	6.3	6.1	5.4	5.2	6.2	6.0
133	27	7.8	5.2	6.7	5.3	6.9	6.5
200	39	6.7	6.2	5.7	3.8	4.1	3.7

Figure 3.4 Mean absolute error (MAE) values between measured TL and TL modeled with BELLHOP. On the left in yellow is the frequency of the sine wave and the approximate reported echo reduction at normal incidence of the echo reducing panels for that given frequency. The values in the green columns are the MAE calculated between the measured data and BELLHOP's predictions. The green columns are grouped by twos based on different water depths and source and receiver depths. The leftmost group is for a measurement taken when $h_w = 0.3$ m, $z_s = h_w/3$, and $z_r = 2h_w/3$. The middle group is when $h_w = 0.3$ m and $z_s = z_r = h_w/2$. The rightmost group is for $h_w = 0.6$ m and $z_s = z_r = h_w/2$. Columns labeled *acrylic* refer to BELLHOP's TL prediction using acrylic parameters for the bottom half-space sound speed and density ($c = 2750$ m/s and $\rho = 1190$ kg/m^3). Columns labeled *optimized* refer to BELLHOP's prediction after Bayesian optimization was done on the MAE varying ρ and c.

3.2 Discussion and Future Work

This work tested if open ocean models BELLHOP and ORCA could model sound propagation in a laboratory water tank when the side walls are lined with echo reducing materials. The best model-data agreement occurs at high frequencies (over 100 kHz) in the deeper water ($h_w = 0.6$ m). Also for the $h_w = 0.6$ m case, several frequencies show good model to data agreement in the first 10 cm centimeters (range $r = 10 - 20$ cm). This agreement could be due to the fact that reflections off the side walls are much closer to normal incidence, the angle that the echo reduction was

BELLHOP and measured data Spearman ρ correlation coefficient							
Frequency (kHz)	Panel loss (dB)	0.3 m, offset		0.3 m, same		0.6 m, same	
		Acrylic	Optimized	Acrylic	Optimized	Acrylic	Optimized
32	34	0.41	0.49	0.48	0.62	0.39	0.45
41	37	0.47	0.49	0.25	0.49	0.25	0.30
53	37	0.35	0.36	0.42	0.38	0.45	0.60
71	40	0.31	0.30	0.35	0.37	0.41	0.39
82	24	0.37	0.48	0.25	0.47	0.44	0.47
100	32	0.40	0.43	0.35	0.37	0.39	0.62
115	43	0.29	0.29	0.39	0.40	0.51	0.53
133	27	0.39	0.55	0.31	0.40	0.34	0.33
200	39	0.21	0.20	0.46	0.72	0.56	0.61

Figure 3.5 Spearman ρ values for the cases described in Fig. 3.4.

ORCA and measured data mean absolute error (dB)										
Frequency (kHz)	Panel loss (dB)	0.3 m, offset			0.3 m, same			0.6 m, same		
		Acrylic	Optimized	Common	Acrylic	Optimized	Common	Acrylic	Optimized	Common
32	34	6.0	5.1	6.9	4.7	4.4	5.3	5.2	4.1	6.1
41	37	5.7	4.9	5.4	5.7	4.5	4.9	6.9	5.5	6.6
53	37	5.5	4.7	5.4	6.1	5.6	6.5	5.0	4.1	5.1
71	40	5.8	5.1	6.5	5.9	5.2	6.5	5.2	4.9	5.4
82	24	6.9	5.0	6.4	6.1	5.4	6.3	5.4	4.7	5.5
100	32	6.2	4.9	6.0	6.6	5.3	6.9	4.5	4.2	4.2
115	43	6.3	5.4	6.9	6.0	5.3	6.4	6.6	6.1	7.6
133	27	8.6	5.9	6.3	7.9	5.5	5.7	6.8	6.4	7.2
200	39	10.1	5.5	10.4	5.5	3.2	3.9	2.9	2.8	2.9

Figure 3.6 Mean absolute error values between measured TL and TL modeled with ORCA. Similar to Fig. 3.4. Columns labeled *acrylic* refer to ORCA's TL prediction using acrylic parameters for the acrylic layer sound speed and density ($c = 2750$ m/s and $\rho = 1.19$ g/cm^3). Columns labeled *optimized* refer to ORCA's prediction after Bayesian optimization was done on the MAE varying ρ and c. Columns labeled *common* refer to common paramters for the acrylic that resulted in low MAE between the measured data and ORCA's predicted TL across all measurements and frequencies. The values chosen were $c = 2200$ m/s and $\rho = 1.8$ g/cm^3.

ORCA and measured data Spearman ρ correlation coefficient										
Frequency (kHz)	Panel loss (dB)	0.3 m, offset			0.3 m, same			0.6 m, same		
		Acrylic	Optimized	Common	Acrylic	Optimized	Common	Acrylic	Optimized	Common
32	34	0.38	0.38	0.21	0.52	0.66	0.44	0.38	0.44	0.24
41	37	0.45	0.54	0.37	0.26	0.54	0.40	0.17	0.34	0.28
53	37	0.35	0.41	0.34	0.35	0.46	0.33	0.47	0.53	0.47
71	40	0.26	0.47	0.42	0.32	0.42	0.28	0.41	0.49	0.55
82	24	0.38	0.58	0.38	0.28	0.41	0.34	0.48	0.51	0.40
100	32	0.37	0.54	0.41	0.36	0.41	0.34	0.59	0.52	0.58
115	43	0.30	0.45	0.32	0.33	0.39	0.26	0.50	0.55	0.61
133	27	0.42	0.54	0.47	0.33	0.44	0.48	0.47	0.45	0.47
200	39	0.30	0.34	0.33	0.49	0.61	0.60	0.91	0.91	0.91

Figure 3.7 Spearman ρ values for the cases described in Fig. **??**.

measured for the side panels. It could be that the panels do not reduce reflections as much at oblique incidences. One future project on this work could be to verify the echo reduction at normal incidence in our tank, and then measure the echo reducing capabilities at more oblique incidences.

The Bayesian optimization did seem to improve model-data agreement, but with seemingly random parameter values. Looking for parameter values manually in the MAE for ORCA was not a reliable way to get better values than the acrylic values found on the ndt.net website [12].

The best model-data agreement is seen with ORCA at 200 kHz at 0.6 m water depth. Because this appears so drastically different than other measurements, it merits further investigation. We have TC4038 hydrophones made by Teledyne that can go up to 500 kHz, so more of these measurements could be taken at frequencies above 200 kHz. The echo reducing panels do not report echo reduction above 200 kHz, but those values could be obtained experimentally in our tank.

Appendix A

Low Frequency Considerations

An unforeseen problem occurred when taking measurements in the tank. The data gathered to investigate that problem are presented along with a possible explanation. Measured transmission loss curves (TL) as a function of range are presented with and without panels.

A.1 Very Shallow Water Regime

As previously mentioned in Sec. 1.2, the shallow water regime is defined as a depth-to-wavelength ratio between 10 and 100. [8] Some of the measurements taken have a depth-to-wavelength ratio below 10, which is referred to as the "very shallow water regime".

To determine the frequency that defines the transition between very shallow water and shallow water, the following equation can be used:

$$f_t = \frac{10 * 1500}{h_w} \tag{A.1}$$

where f_t is the transition frequency, 10 is the minimum depth-to-wavelength ratio, 1500 is the approximate speed of sound in the water, and h_w is the water height. When $h_w = 0.3$ m, f_t = 50 kHz. When $h_w = 0.6$ m,f_t = 25 kHz.

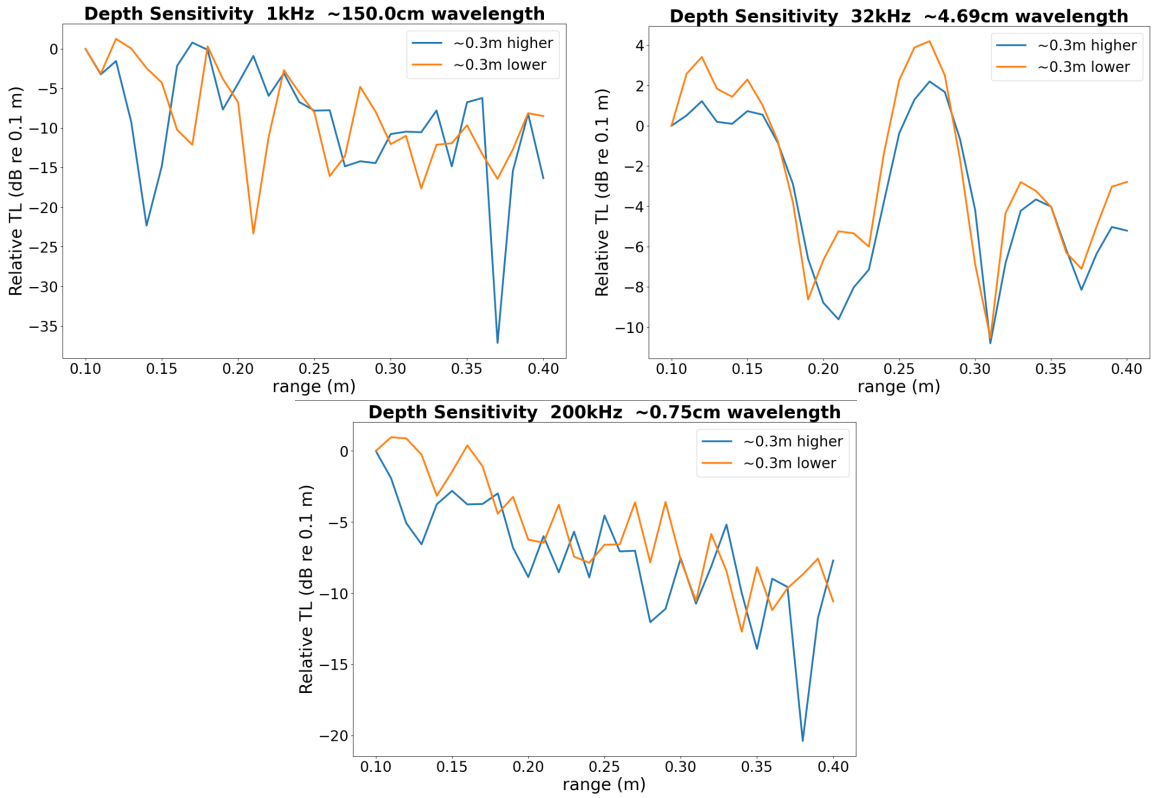

Figure A.1 Variation in measurement after slight change in water depth. The water depth changed by less than one millimeter between measurements. One should expect the 1 kHz TL curve to vary the least because it has the longest wavelength. This does not appear to be the case. The echo-reducing panels were in the tank for these measurements.

During measurements, we noticed that the results of the measured TL values were sensitive to the exact water height. A measurement repeated on a different day gave different results because some of the water had evaporated off the surface. The change in water level was less than 1mm. To investigate this effect we took measurements, drained the tank for 30 seconds (during which time less than 1 mm of water drains), then took the measurement again.

The variation between measurements before and after the tank was drained is shown in Fig. A.1. The plots show TL as a function of range. The frequency and associated wavelength are given in the title. The water height difference is less than 1 mm. The expected variation in measurements should be proportional to the wavelength. The results in Fig. A.1 tell a different story. Even though the

wavelength of a 1 kHz sine wave is five times the depth of the water (i.e. a slight variation in height should make no difference in the transmission loss), the most variation occurs in that measurement. At 32 kHz, the least amount of variation is seen. In order to interpret these graphs, other scenarios need to be considered.

One idea is that our measurements are not repeatable due to time-varying noise in the measurement chain. If we had not drained the tank we still would have gotten a varied result because lack of repeatability. To evaluate this hypothesis, subsequent measurements with the same water level are considered. First the impact of settling time is evaluated with Fig. A.2 showing measurements taken with different settling times. The settling time is how long the computer waits to send the signal after the robots have moved for everything to settle into place. A settling time of 4 seconds had been used because that is how long it took for the water to visually become still again. Maybe this was not long enough, and this motion was adding extra noise into our measurement making them not repeatable. A comparison is shown in Fig A.2 of relative TL when settling times of 4 and 10 s are used (top row), with two different source to receiver range spacing are used: coarse (left) and fine (right). Fig. A.2 shows that the longer settling time doesn't change the TL measurement, so we continued to use 4 s to be more efficient. The second question addressed in Fig. A.2 is whether the robots are really sending the hydrophones to the same place relative to their base time. To test this we repeated the two measurement again, but with five times as many points. The original positions of the previous scans were still used with four extra points in between each one. If those four points are removed, the measurement should still look the same if our measurement taking process is robust. The lower plot in Fig. A.2 shows the resulting relative TL when the water height does not change. The two measurements match well except for a few dB difference at the nulls.

To address why the 32 kHz curve has the least variation in Fig. A.1 we looked to the echo reducing panels in the tank. 32 kHZ is a peak in the echo-reduction chart. Both 200 kHz and 32 kHz reflections should be reduced much better than 1 kHz. That raises the question: is the variability in

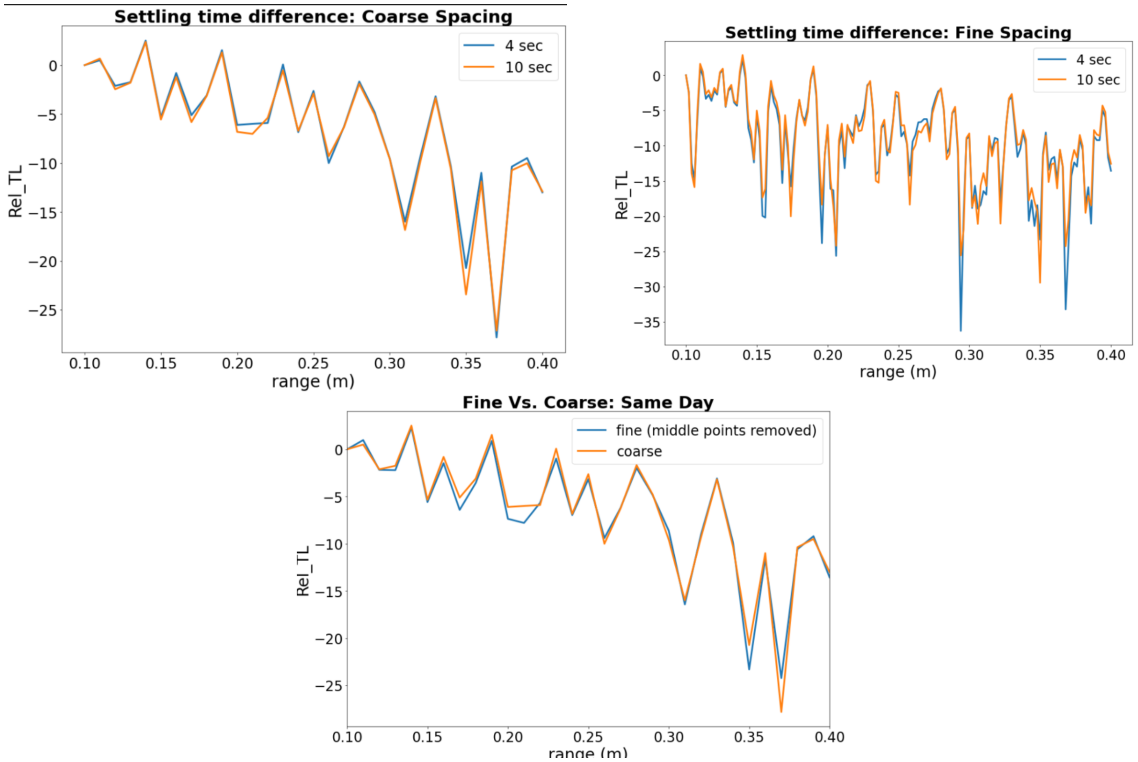

Figure A.2 Proof of repeatability between measurements. This helps show that the variation in Fig. A.1 is caused by the water height change and not chance.

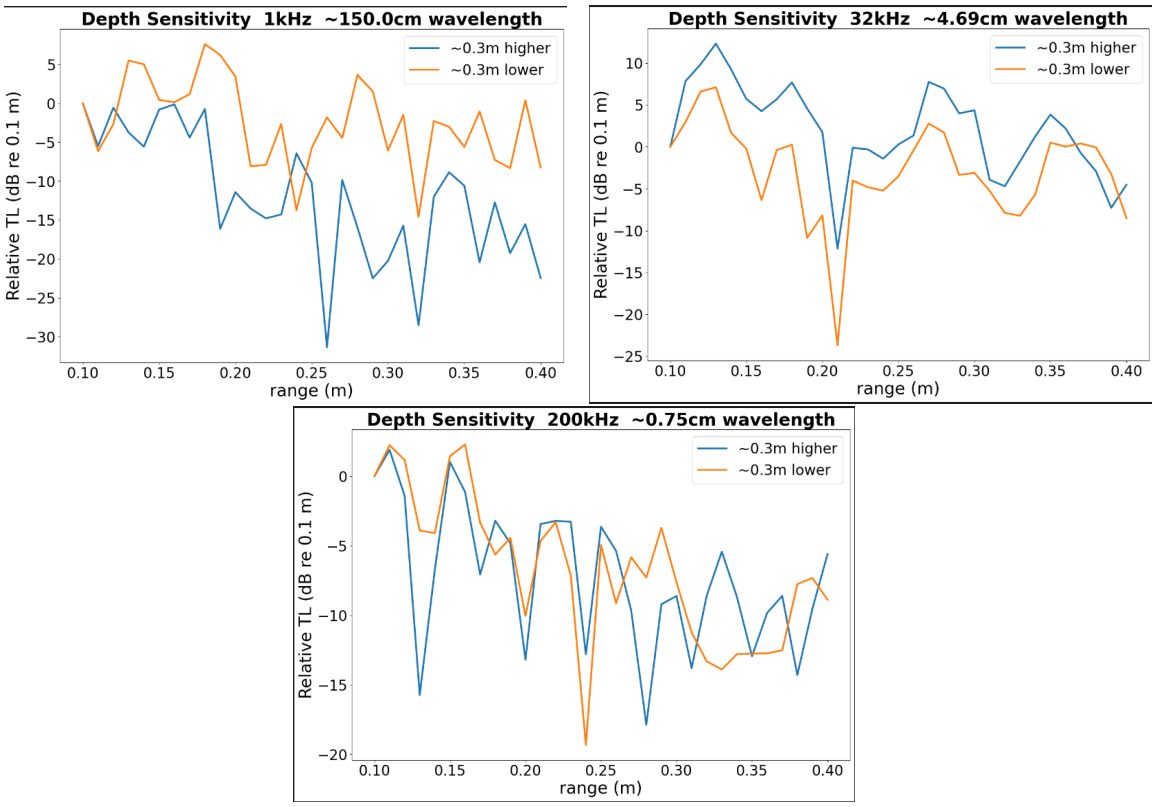

Figure A.3 Results from repeated measurements of those shown in Fig. A.1 but with the panels out of the tank. We still see more variation in the lower frequencies which is puzzling.

measurements with slightly different water heights due to side reflections? To answer this question, the measurements from Fig. A.1 were repeated with the panels taken out of the tank (Fig. A.3). Side reflections should now have a greater impact on the TL for the measurements in Fig. A.3, but it appears that the side reflections are not impacting the variability between TL measured at slightly different water depths. The mechanism behind why there is so much variability at low frequencies is still not known, but we need to exercise caution when taking measurements in the tank in the very shallow water regime.

Appendix B

Supplemental Results

The color density plots for viewing the mean absolute error (MAE) between measured relative TL transmission loss (TL) and values modeled by ORCA as a function of sound speed and density are shown in Figs. B.1, B.2, and B.3. The case of 0.3 m water depth with the source and receiver offset from each other is shown in Fig. B.1. The cases of 0.3 m and 0.6 m with both hydrophones inline with each other at one-half water depth are shown in Figs. B.2 and B.3, respectively. The red dot shows where the Bayesian optimization converged and the yellow dot shows the common parameters that return a low MAE across all cases. The sign of the MAE is flipped (it is now negative) because the `bayesian-optimization` Python package we used maximizes the optimization function. Low MAE refers to bright spots on the plots.

The TL plots for BELLHOP and ORCA using the sound speed (c) and density (ρ) found by the optimizations are compared to the measured TL in Figs. B.4, B.6, and B.8. The common parameter TL plots for ORCA are shown in Figs. B.5, B.7, and B.9. Both sets of figures have the y-axis label removed so that each set of TL curves at one frequency can be labeled. Each grid line represents a 5 dB change and each plot begins at 0 dB.

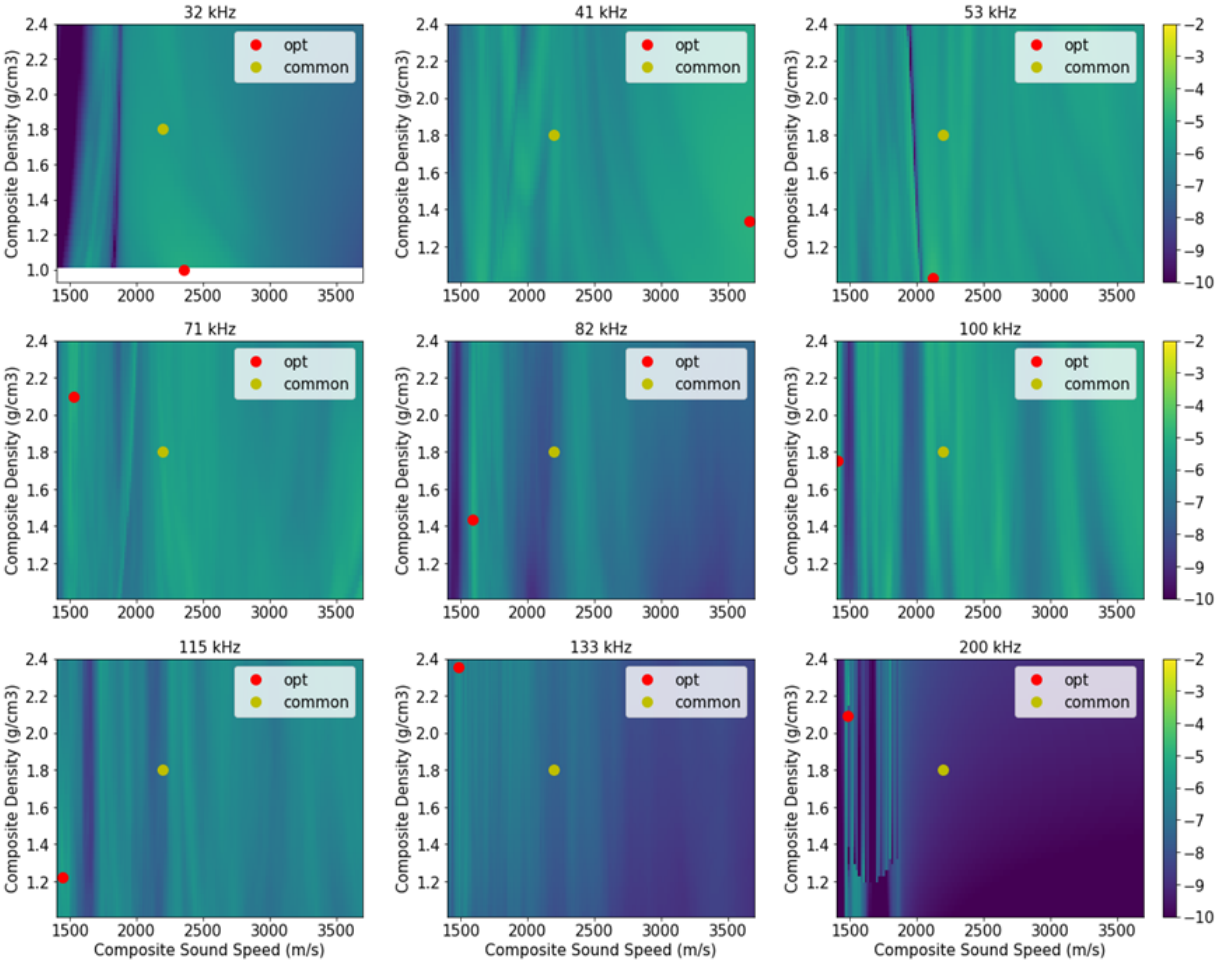

Figure B.1 Color density plot in ORCA parameter space for $h_w = 0.3$ m, $z_s = h_w/3$, and $z_r = 2h_w/3$. Bright colors refer to low MAE while dark colors refer to high MAE. The nine different frequencies for this setup are shown. The red dots show where the Bayesian optimization converged, while the yellow dots show the common parameters chosen for this work ($c = 2200$ m/s and $\rho = 1.8$ g/cm^3).

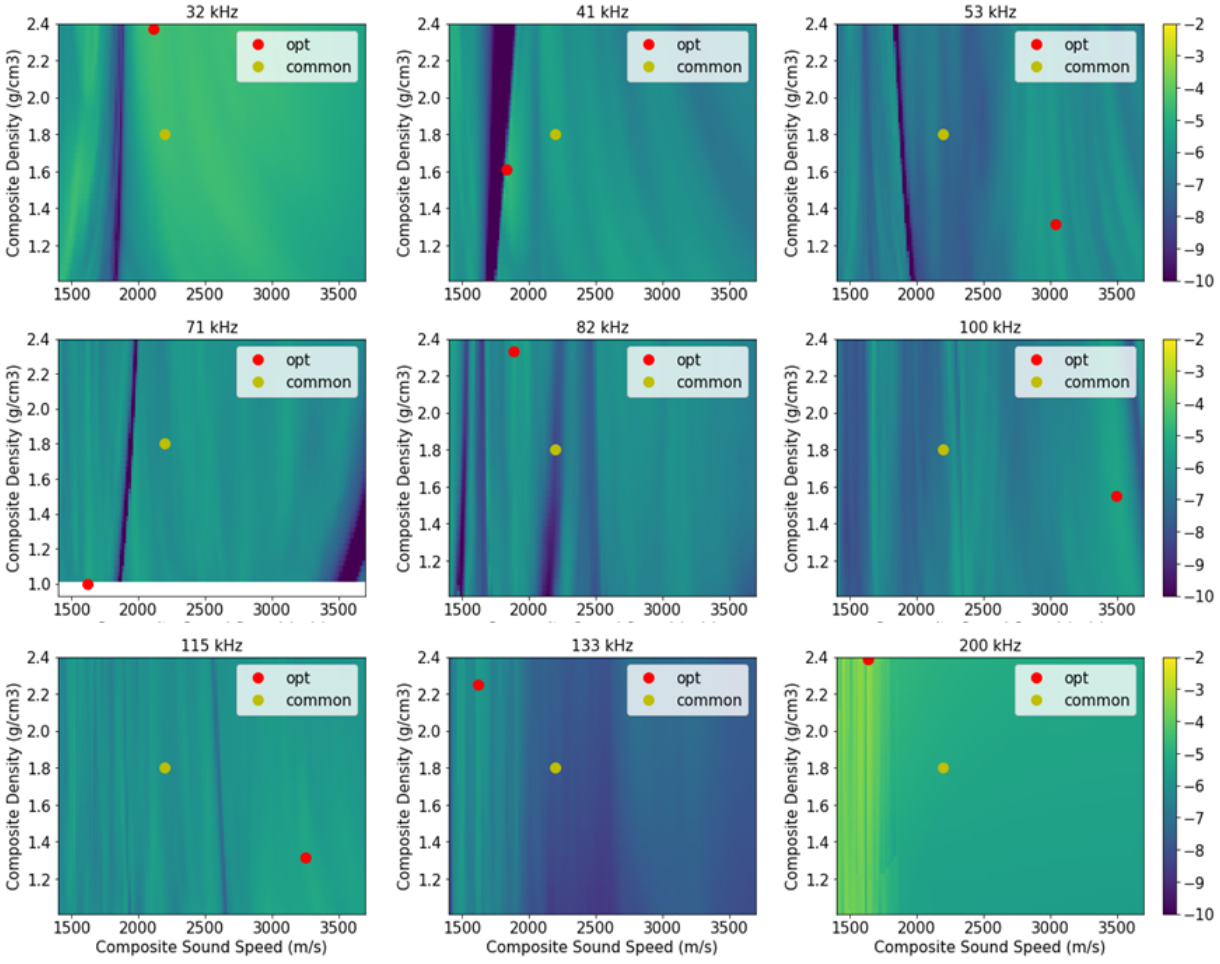

Figure B.2 Similar to Fig. B.1 but for $h_w = 0.3$ m and $z_s = z_r = h_w/2$.

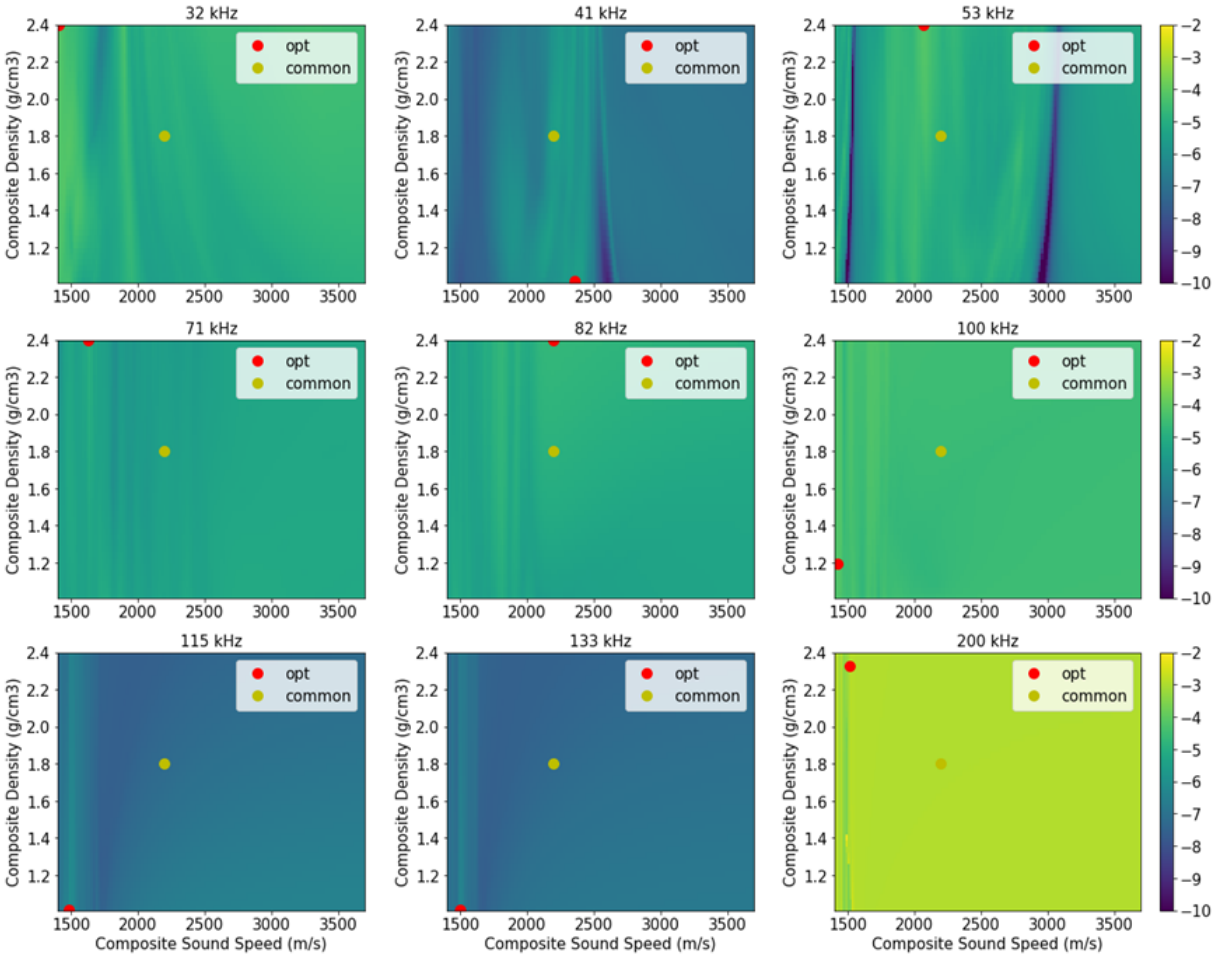

Figure B.3 Similar to Fig. B.1 but for $h_w = 0.6$ m and $z_s = z_r = h_w/2$.

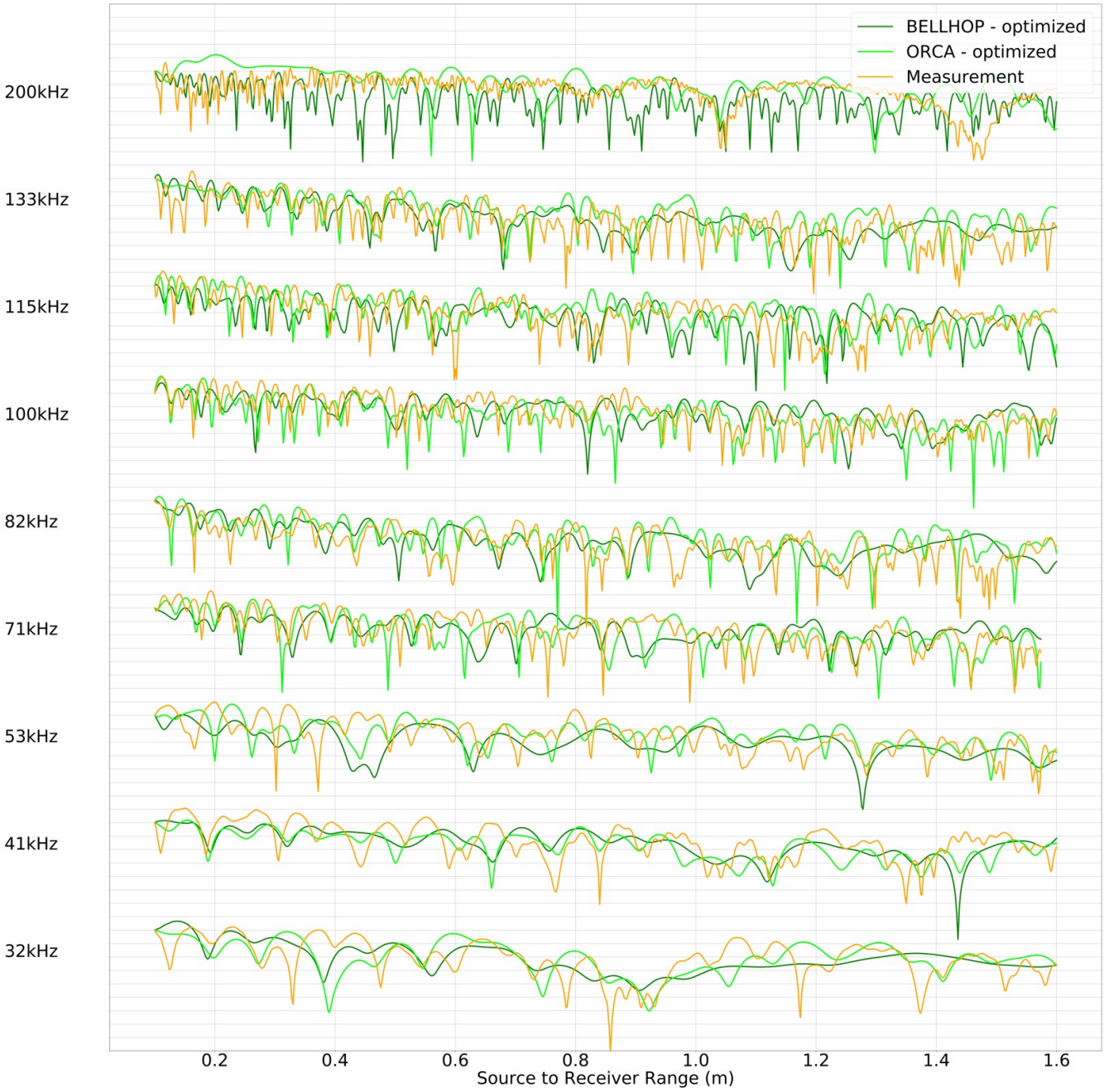

Figure B.4 Transmission loss data sorted by frequency data for $h_w = 0.3$ m, $z_s = h_w/3$, and $z_r = 2h_w/3$. The orange curves show measured TL in the tank. The green curves show TL predicted by BELLHOP and ORCA with parameters found from Bayesian optimization. Gridline separation corresponds to a 5 dB drop in relative transmission loss. The TL curves are relative to the first position of the scan (0.1 meters).

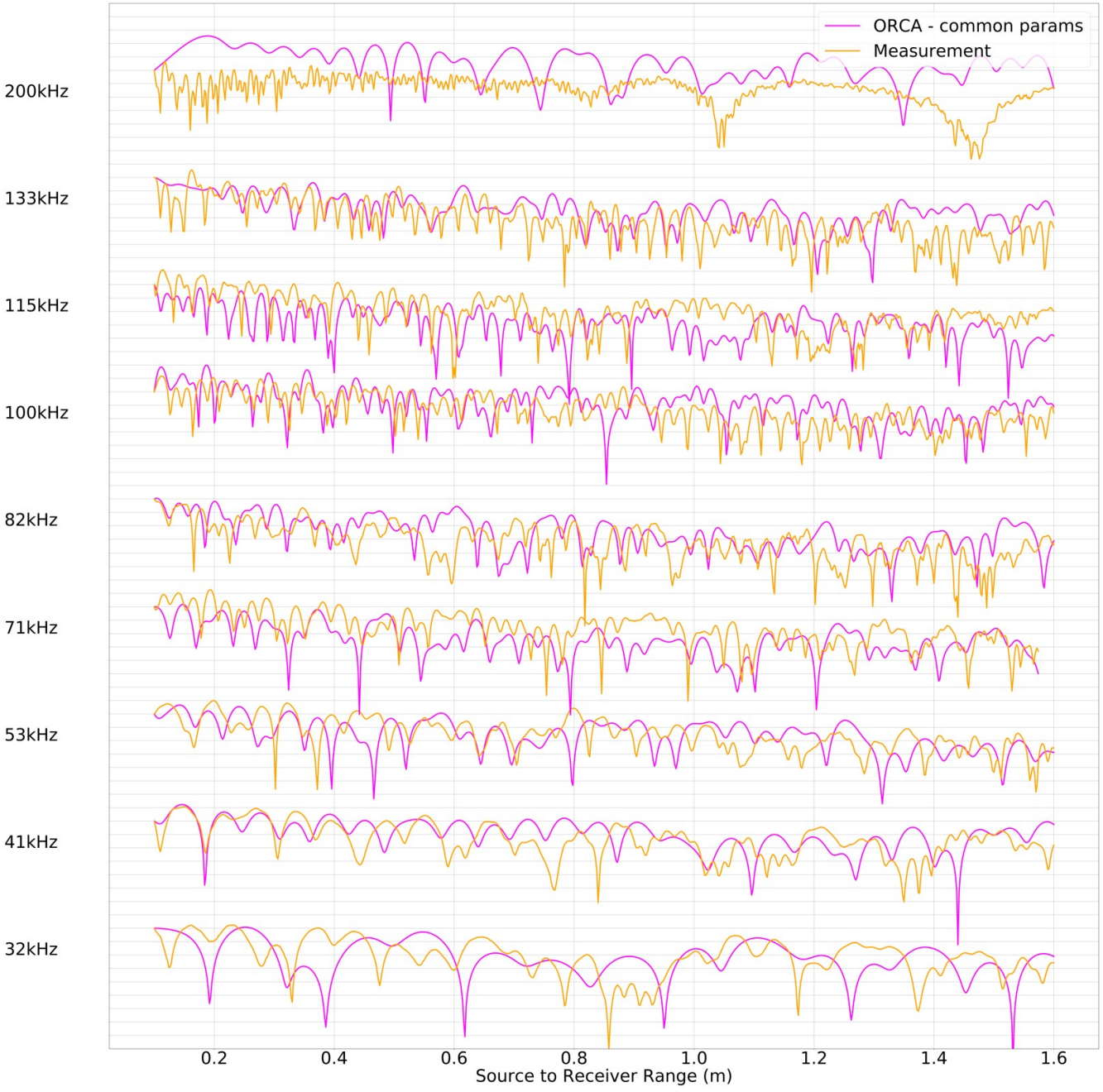

Figure B.5 The pink curves show ORCA's TL prediction with common ORCA parameters ($c = 2200$ m/s and $\rho = 1.8$ g/cm^3). Similar to Fig. B.4.

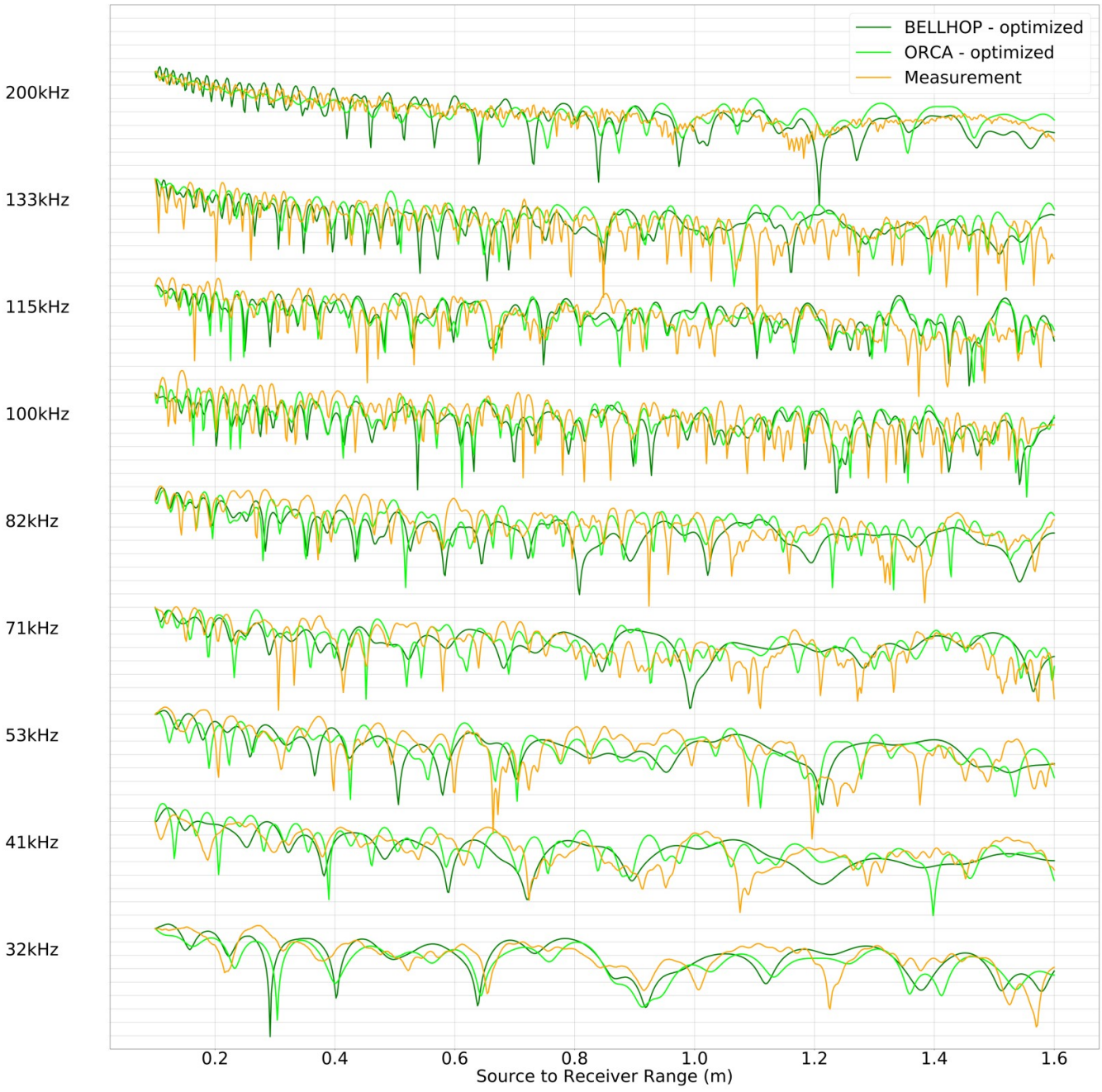

Figure B.6 $h_w = 0.3$ m, $z_s = z_r = h_w/2$. Similar to Fig. B.4.

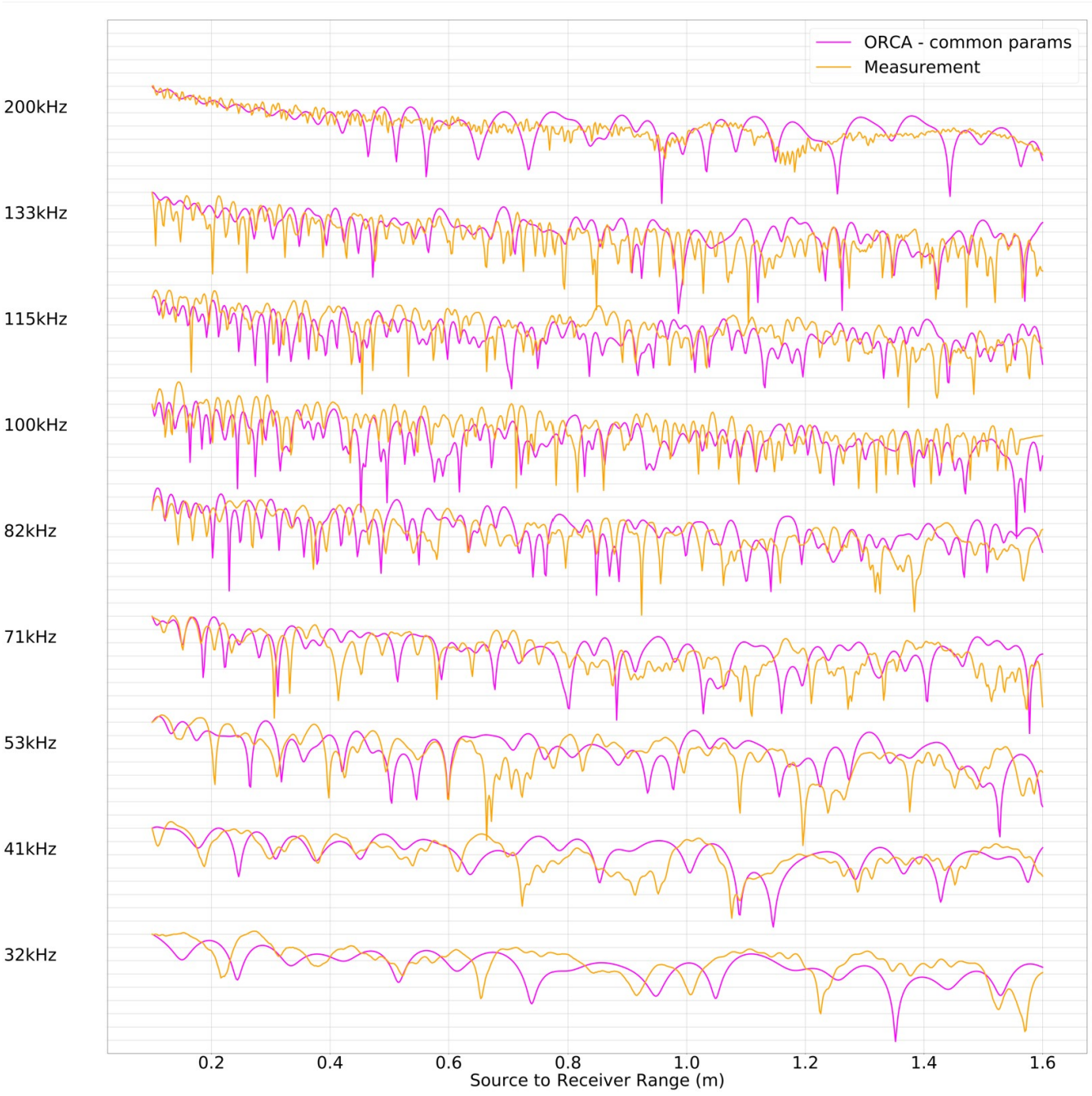

Figure B.7 $h_w = 0.3$ m, $z_s = z_r = h_w/2$. Similar to Fig. B.5.

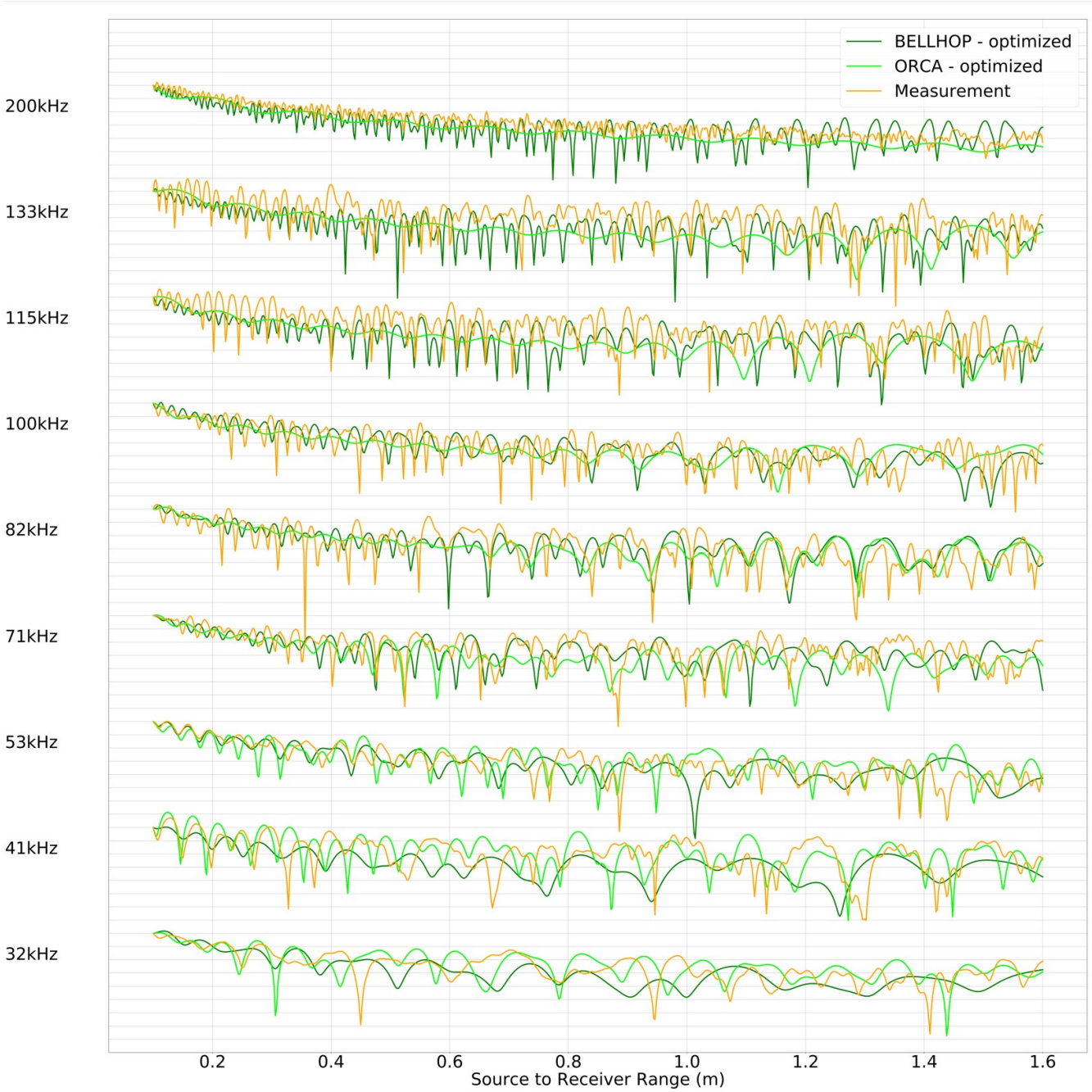

Figure B.8 $h_w = 0.6$ m, $z_s = z_r = h_w/2$. Similar to Fig. B.4.

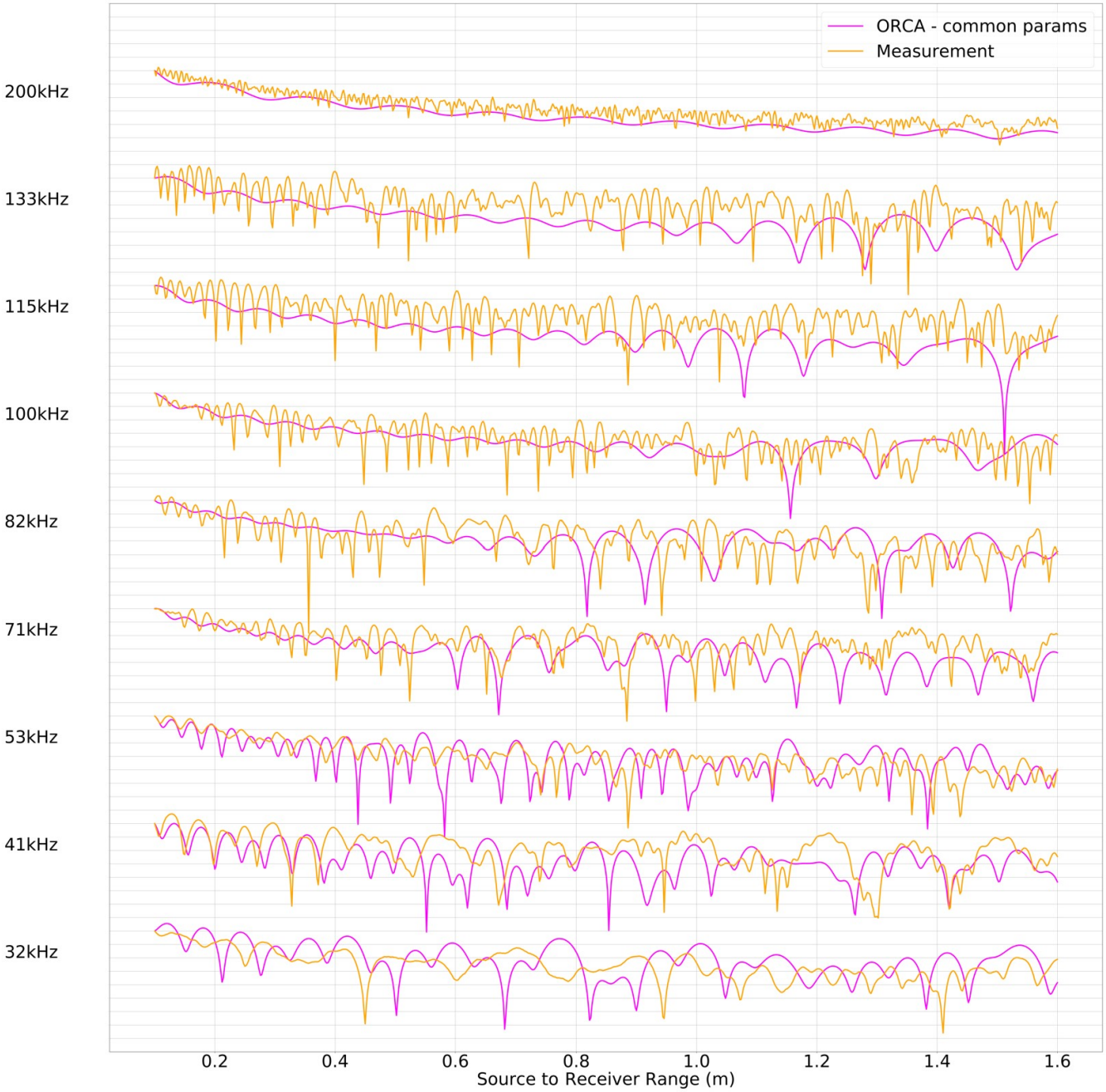

Figure B.9 $h_w = 0.6$ m, $z_s = z_r = h_w/2$. Similar to Fig. B.5.

Appendix C

Code

This section presents all the code used to make the plots in the paper, how to run the code, and where the code is. If the code is run on triton2 or the corner computer in U117 on the sh747 branch in the folder
`mnt/underwater/scott-hollingsworth/codes/`, then the code should run just fine. There may be some adjusting of path names if it is run somewhere else.

The code is split up into two sections: all code that requires BELLHOP to run is in `bellhop-Python/modeling-paper` on the sh747 branch on github. The remaining code is in `uw-measurements/analysis/modeling-paper` on the sh747 branch on github. The code requires that it be run in a certain order that I will describe in the following section.

To recreate Figs. 3.1, 3.2, 3.3, B.4, B.5, B.6, B.7, B.8, and B.9; create plots of a single frequency and setup; and to analyze the Bayesian optimization further run the following code.

C.1 Signal processing and BELLHOP optimization

In `codes/bellhop-Python/modeling` paper open `bayes_opt_bellhop_meas.py`. This code already has the correct paths to data taken for this experiment with additional measurements as well.

In line 68 set the variable called `paths_used` equal to the list of measurements that you wish to run. The current lists are called `same_30`, `same_60`, and `offset_30`. Those currently contain the nine frequencies used in this thesis for the hydrophone setup and water depth (60 or 30 cm). Commented out and above the variables are lists that include a few extra frequencies that were left out of this work. Once that is set, be sure to set the variable `offset` in line 70 to "Offset/" or "Same/" to put it in the correct folder. The water depth is read automatically by the code and placed in the correct folder. If you take a new measurement at a different water depth be sure to make a new folder for it. Also be sure that any new measurements have the full path to it ending in "/". Be sure to save the code once adjustments have been made. Run the code in a tmux session because it will take several hours. The reason the data is broken up into three lists is because you can run three different tmux sessions at once and get it all done in a third the time. If you don't do this it could take days to run. Do not run more than six tmux sessions at once or else one or two will be killed at a random time while the code is running. Once in the tmux session, source the bellhop virtual environment so that the correct packages are downloaded. If you need to create a new virtual environment just run the code, see what package is missing, pip install that package, and then repeat until it can run BELLHOP successfully.

The `bayes_opt_bellhop_meas.py` code will first process the data by removing the leading and trailing zeros, find the autospectral density with the `byuarglib` function `autospec`, sum over the 20 bins surrounding the frequency of the sine wave, and then calculate relative transmission loss. If you want to sum over more or less bins surrounding the frequency of the measurement, then change the variable `plusorminus` on line 102 to a different number. It is currently set to 10 (sums the 10 bins before, the bin with the correct frequency, and the 9 bins after it). After calculating measured relative TL, the code will then run Bayesian optimization to find parameters for the sound speed c and density ρ for the lower half-space that result in the lowest MAE prediction for predicted TL made by BELLHOP and measured TL. The code will save two TL curves made by BELLHOP.

One is the optimized curve and the other is the curve for $c = 2750$ m/s and $\rho = 1190$ kg/m^3. The code also saves a lot of other values that you can look at on lines 253 to 273. This pickle file will be saved in `defaultoutput/Used-in-Paper/Panels` in the respective folder.

There are some potential complications that could arise with the signal processing. This paragraph will only apply for new measurements. And this problem will happen randomly every couple of measurements. It might not be a problem for a new measurement. All measurements currently saved in `bayes_opt_bellhop_meas.py` have been fixed. Sometimes ESAU will record a position incorrectly (an error about the ranges array not being monotonically increasing will probably be returned in this case) or not record a position at all (this will make the ranges array be one value shorter than the `meas_relTL` array). Either way the best way to find the problem is to go into the measurement folder, scroll to the bottom, and open the `scan_positions.txt` file. The columns start with Ægir x, y, and z positions; several columns of zeros; and then Rán positions. The Rán y positions are what the code uses to make the ranges array. Copy and paste the entire file into a spreadsheet. The GT function (greater than) can be used to check if one cell value is greater than the other. This can easily be used to check all 751 cells in the Rán y column. Otherwise you can subtract one cell from another and see if they each y position is incremented by the same amount. Once you find the discrepancy then you can go into the `scan_positions.txt` file, edit it, and save it. Then the code should run just fine. If ESAU didn't save an entire line of the `scan_positions.txt` file then copy a line, paste it in the correct spot, and make sure the correct Rán y value is in saved. The code should run fine after that.

Because the code iterates through several measurements at once in the list, to know which measurement has the issue, you will need to see what the last measurement pickle was that got saved and then find the next one in the list. That is the measurement with the problem. It is best to name your tmux sessions something like `same_60` so you know later that that session ran the `same_60` list for example.

C.2 ORCA optimization

The next code to run after this will do Bayesian optimization for ORCA on all the measurements processed with the previous code. The code is in `uw-measurements/analysis/modeling-paper/` and is called `bayes_opt_orca_meas.py`. This code will read in the pickle files created with the previous code to get the measured data and information about the Bayesian optimization. All the variables related to Bayesian optimization (e.g. `num_iters` or number of iterations) will be read in from the BELLHOP optimization pickle so that it is consistent. If you want to optimize on ORCA differently than you did on BELLHOP then you must manually change those variables.

This code is much easier to run because a lot of things from the previous code were saved in the pickles that this code reads in. Adjust lines 16 and 17 to match the folder you want the ORCA code to iterate through. This should also be done in tmux sessions because it will take a long time. Remember to not run more than six tmux sessions at once.

C.3 ORCA parameter space

This code will recreate the plots in Figs. B.1, B.2, and B.3. The code is in `uw-measurements/analysis/modeling-paper` and is called `parameter_space_orca_bayes.py`. This code does not actually run Bayesian optimization, but instead calculates the optimizing function that the Bayesian optimization used on a fine grid and plots the MAE it returns as a function of sound speed and density. Be sure that the optimizing function used in the BELLHOP optimization and ORCA optimization codes is the same as the one in this file. On top of the parameter space plots for a given frequency and setup, it also plots a red dot where the ORCA optimization ended up. The yellow dot is the common parameters that you will choose. You can comment the yellow dot out (line 124), run the code, look for bright spots where the MAE is a minimum, and find common parameters that will return low MAE for all

frequencies and setups. Once those values are chosen, you can input them into line 124, rerun the code, and verify that that is a good value.

To run the code decide if you want constant color bar bounds or if you want to let them be auto-generated. I would suggest using constant color bar settings. That way if a certain measurement returns high MAE everywhere in parameter space it will all look blue. If the bounds are auto-generated then you will see a bright spot that might look promising, but the MAE is, in fact, not good. To change the bounds edit line 130 or comment it out for auto-generated bounds. The plots in this thesis were all created with constant bounds. There are two save folders if you wish to do both. The save folders are in `defaultoutput/Used-in-Paper-plots` and then there are two subfolders: `const-colorbar` and `vary-colorbar`. Edit line 11 to save the plots to the correct folder. Be sure to edit lines 12 and 13 as well before you run the code. These lines tell you which folders to iterate through. The variables in lines 12 and 13 are missing the '/' unlike the other codes, but this is intentional. Those strings will be added to the image filename and cannot have '/' in them. Run this code in tmux as well because it will take a while. Remember to not run more than 6 tmux sessions at once.

If you don't want to change these plots then you can skip this section, but be sure to rerun the next section anyway.

C.4 Adding ORCA common parameters

The next code to run will iterate through all of the pickles that have been saved up to this point and create and add a relative TL array made by ORCA that use the common parameters gleaned from the plots created by the ORCA parameter space code. The code is in `uw-measurements/analysis/modeling-paper` and is called `common_params_orca.py`. Simply input the common parameters into lines 64 and 65 and run the code. Because this code runs so

quickly it does not need to be broken up into chunks, so there is no need to put in the folder you want to iterate through. It will iterate through all folders and add a `common_orca_relTL` array to all the ORCA pickles. No need to use tmux. It should run in a few minutes.

There used to be a BELLHOP common parameters code, but it is now in an old folder because it was not used for this paper. If you want to try to find common BELLHOP parameters you can try to use it but I cannot guarantee this code will run the first time. It might need to be edited slightly. It is in `bellhop-Python/modeling-paper/old` and is called `common_params_bellhop.py`. BELLHOP uses composite lower half-space parameters so they might be a function of frequency. So, you will need to take several measurements at a single frequency with different water depths, source depths, and receiver depths and try to find common parameters from those measurements. In my opinion, this would be a waste of time.

If you skipped the previous section, rerun this section anyway because they new pickles created by `bayes_opt_bellhop_meas.py` and `bayes_opt_orca_meas.py` do not create the common parameter TL array.

C.5 Combining pickles, creating Plots, and analyzing Bayesian optimization

The remaining code must be done on the corner computer in U117 locally in Spyder (not on triton2). This is because it will be saving large figures. That computer can access Box and the W drive simultaneously. The figures will be saved on Box because there is more space for big files.

The code is in `uw-measurements/analysis/modeling-paper` and is called `combinepickles_modeldataplots_bayesanalysis.py`. The first step is to run the first cell called Block 1. To run a single cell in Spyder just hit `Shift+Enter` when the text cursor (blinking solid line that shows where you will type next) is in the cell you want to run. No need to change

anything about this cell. It combines the ORCA pickles and BELLHOP pickles on the W drive and saves the new one on Box in `Underwater Measurements/Scott Hollingsworth/Modeling Paper Pickles/Used-in-Paper`.

Next you can run Block 2. This will recreate Figs. 3.1, 3.2, 3.3, B.4, B.5, B.6, B.7, B.8, and B.9 and create plots of a single frequency and setup. It generates several plots and will take several minutes. It can also create those same plots but have ranges in units of wavelength on the x-axis instead of meters. Those plots are not included in this thesis. This block of code will also create spreadsheets with all the metrics in them. These tables were used to create Figs. 3.4, 3.5, 3.6, and 3.7. To make them into nice looking tables will require some effort, but everything you need will be saved in spreadsheets. Each spreadsheet has two sheets in it, one labeled BELLHOP and one labeled ORCA. The spreadsheets and figures are all saved in Box under
`Underwater Measurements/Scott Hollingsworth/Modeling Paper Plots/Used-in-Paper`

Block 3 is used if you want to analyze the Bayesian optimization. This block was not used to create anything in this thesis, but it can be helpful when trying to analyze the data. This will only run for one measurement. Input the measurement you want into lines 362-364 and run the cell. It will produce some plots and print some information, but not save anything.

C.6 Water Sensitivity Plots

This section is to help recreate Figs. A.1, A.2, and A.3. These plots will probably not need to be recreated, but the paths to the measured data and process for recreating them are recorded here. The data is stored on the W drive in `uw-measurements-tank/2022/2022-11-30`. Follow the lab manual word doc in that folder to find the measurements taken at 1 kHz, 32 kHz, and 200 kHz. To make the plots go onto the github `uw-measurements/analysis` repository, sh747 branch, and back to the code pushed on November ninth, 2022. The name of the file is `check_freq.py`. That

file will need to be adjusted in order to get it to produce the exact plots in this thesis.

Bibliography

[1] "Acoustics Toolbox," http://oalib.hlsresearch.com/AcousticsToolbox/ (Accessed June 9, 2023).

[2] E. K. Westwood, C. T. Tindle, and N. R. Chapman, "A normal mode model for acousto-elastic ocean environments," The Journal of the Acoustical Society of America **100,** 3631–3645 (1996).

[3] F. Jensen, W. Kuperman, M. Porter, and H. Schmidt, *Computational Ocean Acoustics* (Springer Science+Business Media, 233 Spring Street, New York, USA, 2011).

[4] "50 Part A Propagation of Sound,".

[5] C. Vongsawad, "Development and Characterization of an Underwater Acoustics Development and Characterization of an Underwater Acoustics Laboratory Via in situ Impedance Boundary Measurements Laboratory Via in situ Impedance Boundary Measurements BYU ScholarsArchive Citation BYU ScholarsArchive Citation,", 2021.

[6] D. C. Baumann, J. M. Brendly, D. B. Lafleur, P. L. Kelley, R. L. Hildebrand, and E. I. Sarda, "Techniques for Scaled Underwater Reverberation Measurements,".

[7] P. Papadakis, M. Taroudakis, F. Sturm, P. Sanchez, and J. P. Sessarego, "Scaled laboratory experiments of shallow water acoustic propagation: Calibration phase," Acta Acustica united with Acustica **94,** 676–684 (2008).

[8] W. A. Kuperman and J. F. Lynch, "Shallow-water acoustics," Physics Today **57,** 55–61 (2004).

[9] H. Kim, B. Gutierrez, T. Nelson, A. Dumars, M. Maza, H. Perales, and G. Voulgaris, "Using the acoustic Doppler current profiler (ADCP) to estimate suspended sediment concentration," University of South Carolina pp. 04–01 (2004).

[10] A. Novak, M. Bruneau, and P. Lotton, "Small-sized rectangular liquid-filled acoustical tank excitation: A modal approach including leakage through the walls," Acta Acustica united with Acustica **104,** 586–596 (2018).

[11] K. N. Terry, C. T. Vongsawad, and T. B. Neilsen, "Cartesian normal-mode models for a mid-size laboratory water tank," In *Proceedings of Meetings on Acoustics 181ASA*, **45,** 070007 (2021).

[12] R. Diederichs, "Plastic Material's acoustic properties," https://www.ndt.net/links/proper.htm (Accessed June 9, 2023).

Index